

# Feature Extraction Approaches for Biological Sequences: A Comparative Study of Mathematical Models

Robson Parmezan Bonidia<sup>a,b,\*</sup>, Lucas Dias Hiera Sampaio<sup>a</sup>, Douglas Silva Domingues<sup>a</sup>, Alexandre Rossi Paschoal<sup>a</sup>, Fabrício Martins Lopes<sup>a</sup>, André Carlos Ponce de Leon Ferreira de Carvalho<sup>b</sup>, Danilo Sipoli Sanches<sup>a</sup>

<sup>a</sup>*Department of Computer Science, Bioinformatics Graduate Program (PPGBIOINFO), Federal University of Technology - Paraná, UTFPR, Campus Cornélio Procópio, Brazil.*

<sup>b</sup>*Institute of Mathematics and Computer Sciences, University of São Paulo - USP, São Carlos, 13566-590, Brazil*

---

## Abstract

The number of available biological sequences has increased significantly in recent years due to various genomic sequencing projects, creating a huge volume of data. Consequently, new computational methods are needed to analyze and extract information from these sequences. Machine learning methods have shown broad applicability in computational biology and bioinformatics. The utilization of machine learning methods has helped to extract relevant information from various biological datasets. However, there are still several obstacles that motivate new algorithms and pipeline proposals, mainly involving feature extraction problems, in which extracting significant discriminatory information from a biological set is challenging. Considering this, our work proposes to study and analyze a feature extraction pipeline based on mathematical models (Numerical Mapping, Fourier, Entropy, and Complex Networks). As a case study, we analyze Long Non-Coding RNA sequences. Moreover, we divided this work into two studies, e.g., (I) we assessed our proposal with the most addressed problem in our review, e.g., lncRNA vs. mRNA; (II) we tested its generalization on different classification problems, e.g., circRNA vs. lncRNA. The experimental results demonstrated three main contributions: (1) An in-depth study of several mathematical models;

---

\*Corresponding author

*Email addresses:* [rpbonidia@gmail.com](mailto:rpbonidia@gmail.com) (Robson Parmezan Bonidia), [danielosanches@utfpr.edu.br](mailto:danielosanches@utfpr.edu.br) (Danilo Sipoli Sanches)

(2) a new feature extraction pipeline and (3) its generalization and robustness for distinct biological sequence classification.

*Keywords:* Feature Extraction; Long Non-Coding RNAs; Biological Sequences; Numerical Mapping Techniques; Fourier; Complex Networks; Shannon; Tsallis.

---

## 1. Background

In recent years, due to advances in DNA sequencing, an increasing number of biological sequences have been generated by thousands of sequencing projects [1], creating a huge volume of data [2]. During the last decade, Machine Learning (ML) methods have shown broad applicability in computational biology and bioinformatics [3]. Consequently, the ability to process and analyze biological data has advanced significantly [4]. Tools have been applied in gene networks, protein structure prediction, genomics, proteomics, protein-coding genes detection, disease diagnosis, and drug planning [5, 6]. Fundamentally, ML investigates how computers can learn (or improve their performance) based on the data. Moreover, ML is a specialization of computer science related to pattern recognition and artificial intelligence [7].

Based on this, several works have focused on investigating sequences of DNA and RNA molecules [8, 9, 10]. Applying ML methods in these sequences has helped to extract important information from various datasets to explain biological phenomena [3]. The development of efficient approaches benefits the mathematical understanding of the structure of biological sequences [1], e.g., Precision cancer diagnostics [11], analytics in plants [12], and Coronavirus epidemic [13, 14]. However, according to [3, 15], there are still several challenging biological problems that motivated the emergence of proposals for new algorithms. Fundamentally, biological sequence analysis with ML presents one major problem, e.g., Feature Extraction [16], an inevitable process, especially in the stage of biological sequence preprocessing [10, 17].

Feature extraction seeks to generate a feature vector, optimally transforming the input data [16]. This procedure is exceptionally relevant for the success of the ML application because another primary goal is to extract important information from input data compactly, as well as removing noise and redundancy to increase the accuracy of ML models [18, 16]. Necessarily, several methods in bioinformatics apply ML algorithms for sequence classification, and as many algorithms can deal only with numerical data, sequences

31 need to be translated into sequences of numbers.

32 Thereby, modern applications extract relevant features from sequences  
33 based on several biological properties, e.g., physicochemical, Open Reading  
34 Frames (ORF)-based, usage frequency of adjoining nucleotide triplets, GC  
35 content, among others. This approach is common in biological problems, but  
36 these implementations are often difficult to reuse or adapt to another specific  
37 problem, e.g., ORF features are an essential guideline for distinguishing Long  
38 non-coding RNAs (lncRNA) from protein-coding genes [19], but not useful  
39 features for classifying lncRNA classes [20, 21] (e.g., in [21], ORF score (fea-  
40 ture importance) is less than 0.009 to classify circular RNA from other types  
41 of lncRNAs). Consequently, the feature extraction problem arises, in which  
42 extracting a set of useful features that contain significant discriminatory in-  
43 formation becomes a fundamental step in the construction of a predictive  
44 model [22].

45 Therefore, these problems make the process of biological sequence clas-  
46 sification a challenging task, creating a growing need to develop new tech-  
47 niques and methods to analyze sequences effectively and efficiently. Thereby,  
48 this work studies the performance of different feature extraction methods  
49 for biological sequence analysis, using mathematical models, e.g., numerical  
50 mapping, Fourier transform, entropy, and graphs. As a case study, we will  
51 use lncRNA sequences, which are fundamentally unable to produce proteins  
52 [23] and have recently casted doubt on its functionality [24].

53 lncRNAs present several problem classes (e.g., lncRNA vs. mRNA [25,  
54 26] and lncRNA vs. circRNA [27]), thus enabling us to create a scenario to  
55 answer the questions raised in this work. Fundamentally, our main objective  
56 is to propose generalist techniques, demonstrating their efficiency concerning  
57 biological features. We consider biological approaches, those characteristics  
58 that present a bias to the analyzed problem or some biological explanation,  
59 e.g., ORF for lncRNA vs. mRNA [6, 19], as well as mathematical approaches  
60 and information quantity measures such as entropy. Based on this context  
61 and objectives, we assume the following hypothesis:

- 62 • **Hypothesis:** Feature extraction approaches based on mathematical  
63 models are as efficient and generalist as biological approaches.

64 Considering this, our work contributes to the area of computer science  
65 and bioinformatics. Specifically, it introduces new ideas and analysis for  
66 the feature extraction problem in biological sequences. Thereby, we present

67 four new contributions: (1) A feature extraction pipeline using mathematical  
68 models; (2) Analysis of 9 mathematical models; (3) Analysis of 6 numerical  
69 mappings with Fourier, proposing statistical characteristics; (4) The general-  
70 ization and robustness of mathematical approaches for the feature extraction  
71 in biological sequences.

## 72 2. Related Works

73 Essentially, as emphasized, we adopt lncRNA sequences as a case study,  
74 a class of Non-Coding RNAs (ncRNAs). Fundamentally, ncRNAs are un-  
75 able to produce proteins. However, these ncRNAs contain unique informa-  
76 tion that produces other functional RNA molecules [28, 23]. Moreover, they  
77 demonstrate essential roles in cellular mechanisms, playing regulatory roles  
78 in a wide variety of biological reactions and processes [29, 28]. The ncR-  
79 NAs can be classified by length into two classes: Long Non-Coding RNA  
80 (lncRNA - 200 nucleotides (nt) or more) and short ncRNA (less than 200  
81 nt) [30, 31]. The lncRNAs are sequences with a length greater than 200 nu-  
82 cleotides [32], and according to recent studies, play essential roles in several  
83 critical biological processes [33, 34, 35], including transcriptional regulation  
84 [36], epigenetics [37], cellular differentiation [38], and immune response [39].  
85 Moreover, they are correlated with some complex human diseases, such as  
86 cancer and neurodegenerative diseases [6, 40, 41].

87 In plants, according to [6, 42], the lncRNAs act in gene silencing, flowering  
88 time control, organogenesis in roots, photomorphogenesis in seedlings, stress  
89 responses [43, 44], and reproduction [45]. Furthermore, lncRNAs are present  
90 in large numbers in genome [46] and have similar sequence characteristics  
91 with protein-coding genes, such as 5' cap, alternative splicing, two or more  
92 exons [47], and polyA+ tails [48]. They are also observed in almost all living  
93 beings, not only in animals and plants but also yeasts, prokaryotes, and even  
94 viruses [49, 50].

95 According to [46], lncRNAs do not contain functional ORFs. However,  
96 recent studies have found bifunctional RNAs [51], raising the possibility that  
97 many protein-coding genes may also have non-coding functions. Further-  
98 more, lncRNAs can be grouped into five broad categories. The classifi-  
99 cation occurs conforming to the genomic location, that is, where they are  
100 transcribed, concerning well-established markers, e.g., protein-coding genes.  
101 Among the categories are [52, 47]: sense, antisense, bidirectional, intronic,  
102 intergenic. The genomic context does not necessarily provide some informa-

103 tion about the lncRNAs function or evolutionary origin; nevertheless, it can  
104 be used to organize these broad categories [53].

105 In this context, we have conducted an in-depth review of the lncRNAs  
106 classification methods, in which several approaches have been developed,  
107 such as: CPC [54], CPAT [55], CNCI [56], PLEK [57], lncRNA-MFDL  
108 [58], LncRNA-ID [59], lncRScan-SVM [60], LncRNAPred [61], DeepLNC  
109 [62], PlantRNA\_Sniffer [63], PLncPRO [64], RNAPlong [65], BASiNET [66],  
110 LncFinder [26], CREMA [67], LncRNAnet [19], CNIT [68], PLIT [69], PredLnc-  
111 GFStack [70], LGC [71] and DeepCPP [72]. For better understanding, Figure  
112 1 presents these works divided into Mathematical, Biological, and Hybrid  
113 approaches.

114 The CPC uses the extent and quality of the ORF, and derivation of the  
115 BLASTX [73] search to measure the protein-coding potential of a transcript.  
116 In the classification, the authors applied the LIBSVM package to train a Sup-  
117 port Vector Machine (SVM) model, using the standard radial basis function  
118 kernel. CPAT classifies transcripts of coding and non-coding using the Logis-  
119 tic Regression (LR) classifier. This approach implements four features: ORF  
120 coverage, ORF size, hexamer usage bias, and Fickett TESTCODE statis-  
121 tic. CNCI was induced with SVM and applies profiling Adjoining Nucleotide  
122 Triplets, and most-like CDS (MLCDS).

123 In contrast, PLEK (2014) is based on the k-mer scheme ( $k = 1, \dots, 5$ )  
124 to predict lncRNA, also applying the SVM classifier. lncRNA-MFDL uses  
125 Deep Learning (DL) and multiple features, among them: ORF, K-mer ( $k =$   
126  $1, 2, 3$ ), secondary structure (minimum free energy), and MLCDS. LncRNA-  
127 ID predicts lncRNAs with Random Forest (RF) through ORF (length and  
128 coverage), sequence structure (Kozak motif), ribosome interaction, alignment  
129 (profile Hidden Markov Mode - profile HMM), and protein conservation.

130 lncRScan-SVM uses stop codon count, GC content, ORF (score, CDS  
131 length and CDS percentage), transcript length, exon count, exon length, and  
132 average PhastCons scores. LncRNAPred classified lncRNAs with RF and  
133 features based on ORF, signal to noise ratio, k-mer ( $k = 1, 2, 3$ ), sequence  
134 length, and GC content. DeepLNC uses only the k-mer scheme with entropy  
135 and Deep Neural Network (DNN). PlantRNA\_Sniffer was developed in 2017  
136 to predict Long Intergenic Non-Coding RNAs (lincRNAs). The method ap-  
137 plied SVM and extracted features from ORF (proportion and length) and  
138 nucleotide patterns.

139 PLncPRO is based on machine learning and uses RF. The features se-  
140 lected include ORF quality (score and coverage), number of hits, significance

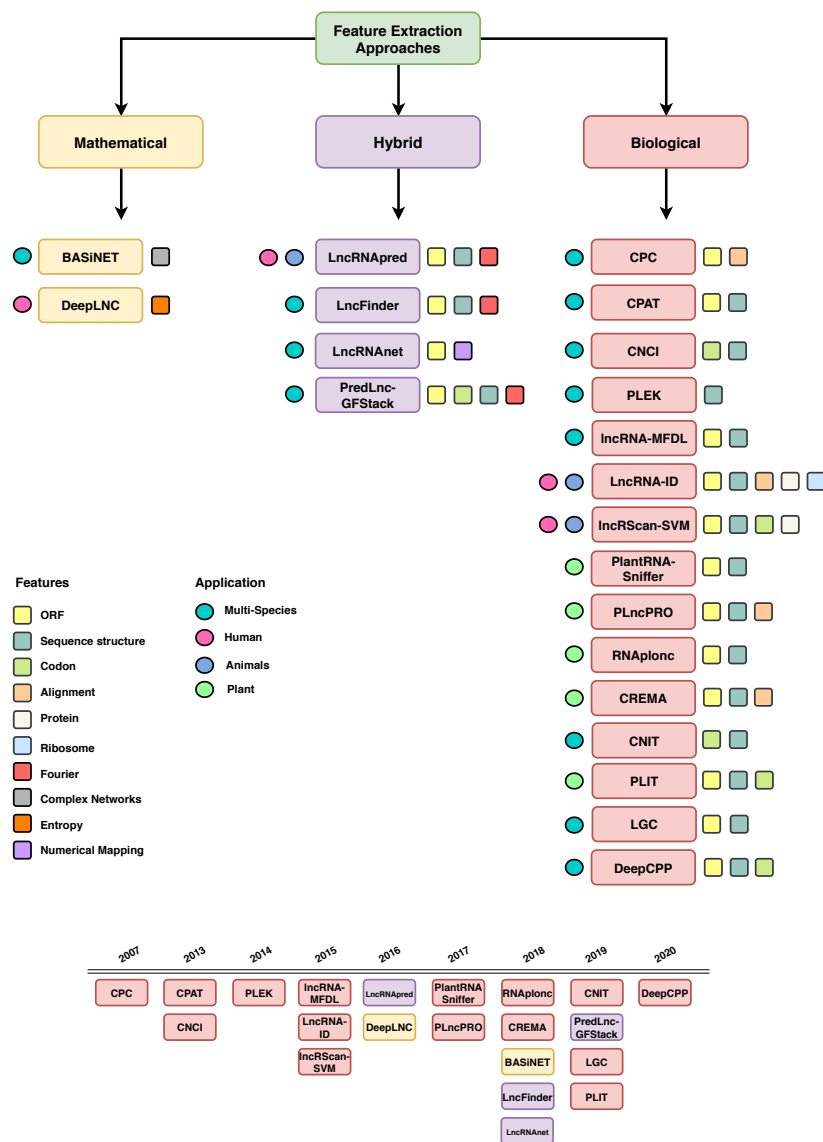


Figure 1: Feature extraction approaches in our case study divided into: Mathematical, Biological, and Hybrid.

141 score, total bit score, and frame entropy. RNAplonc classified sequences with  
 142 the REPTree algorithm, considering 16 features (ORF, GC content, K-mer  
 143 scheme ( $k = 1, \dots, 6$ ), sequence length). BASiNET classifies sequences based  
 144 on the feature extraction from complex network measurements. LncFinder

145 tests five classifiers (LR, SVM, RF, Extreme Learning Machine, and Deep  
146 Learning), to apply the algorithm that obtains the highest accuracy. The  
147 authors extract features from ORF, secondary structural, and EIIP-based  
148 physicochemical properties.

149 CREMA uses ensemble machine learning classifiers. Features include  
150 mRNA length, ORF (length), GC content, Fickett score, hexamer score,  
151 alignment, transposable element, and sequence percent divergence from a  
152 transposable element. LncRNA-net applies a deep learning-based approach  
153 using numerical mapping and ORF indicators. CNIT is the updated CNCI  
154 tool with a novel approach (XGBoost models with adjoining nucleotide triplets  
155 and MLCDS). PLIT is a new alignment-free tool that uses ORF, transcript  
156 length, Fickett score, Hexamer Score, GC content, and codon-bias features.

157 Lastly, PredLnc-GFStack also uses the stacked ensemble learning method  
158 by extracting features based on codon-bias, Fickett score, ORF, GC content,  
159 coding sequence, transcript length, k-mer, CTD, Hexamer score, signal to  
160 noise ratio, UTR coverage, EDP of transcripts (entropy density profiles)  
161 and structure-related. LGC proposes a feature relationship-based approach  
162 (ORF length and GC content). DeepCPP is a deep learning method for  
163 RNA coding potential prediction. Among the extracted features are ORF,  
164 hexamer score, Fickett score, k-mer, g-gap, and nucleotide bias.

165 In general, the aforementioned works apply supervised learning methods  
166 using binary classification (two classes - lncRNAs and protein-coding genes  
167 (mRNA)). There is a considerable amount of research on humans, followed  
168 by animals and plants. Regarding feature extraction, we observed a full do-  
169 main of ORF and sequence-structure descriptors. As seen in Figure 1, there  
170 is a frequent use of biological features. On the other hand, some works have  
171 explored mathematical approaches for feature extraction, such as Genomic  
172 Signal Processing (GSP), DNA Numerical Representation (DNR) [61, 26],  
173 and Complex Networks [66]. Nevertheless, the authors used these charac-  
174 teristics in conjunction with other biological feature extraction techniques  
175 or without testing other mathematical features. Practically no papers have  
176 focused on several mathematical approaches. Based on this, the objective of  
177 this section was to summarize the main methods of the literature and their  
178 characteristic descriptors. Therefore, we will not use the works shown for  
179 comparison, but the most applied features.

### 180 3. Materials and Methods

181 In this section, we describe the methodological approach used to achieve  
182 the proposed objectives, as shown in Figure 2. Essentially, we divided our  
183 study into five stages: (1) Data selection and preprocessing; (2) Feature  
184 extraction; (3) Training; (4) Testing; (5) Performance analysis. Hence, each  
185 stage of the study is described, as well as information about the adopted  
186 process.

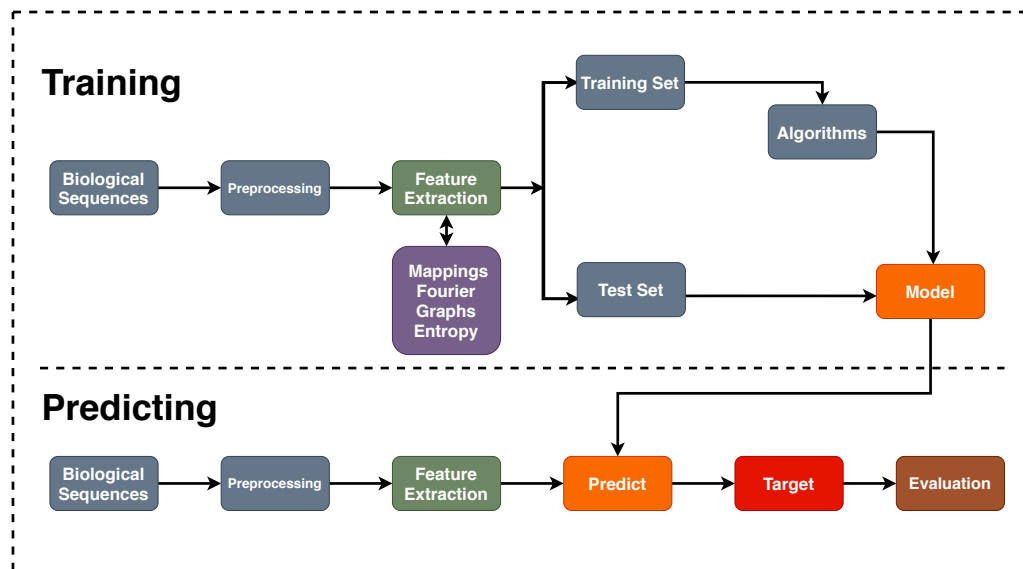


Figure 2: Proposed Pipeline. Essentially, (1) datasets are preprocessed; (2) Feature extraction techniques are applied to each dataset; (3) Machine learning algorithms are executed in the training set to induce predictive models; (4) Induced models are applied to the test set; Finally, (5) the models are evaluated.

187 This work was also divided into two case studies: (I) We assessed our  
188 mathematical approaches with the most addressed problem in our review,  
189 e.g., lncRNA vs. mRNA; (II) We tested its generalization on different clas-  
190 sification problems.

#### 191 3.1. Data Selection

192 As previously mentioned, we chose the lncRNAs classification problem,  
193 because it is a new and relevant theme in the literature, in which, recently,  
194 it has presented several works, mainly with ML, as explored in Section 2.



195 However, we will also adopt other datasets to assess the generalization of  
196 mathematical features. As preprocessing, we used only sequences longer  
197 than 200nt [57], and we also removed sequence redundancy. Moreover, the  
198 sampling method was adopted in our dataset, since we are faced with the  
199 *imbalanced data problem* [20]. Therefore, we applied random majority under-  
200 sampling, which consists of removing samples from the majority class (to  
201 adjust the class distribution) [74]. Finally, we divided this paper into two  
202 case studies.

### 203 3.1.1. Case Study I

204 Sequences of five plant species were adopted to validate the proposed  
205 approaches. The summary of the dataset can be seen in Table 1. According to  
206 the literature approaches, this study also adopts two classes for the datasets:  
207 the positive class, with lncRNAs, and the negative class, with protein-coding  
208 genes (mRNAs).

Table 1: Adopted species to create the datasets.

Species	Sequences	Samples	Preprocessing	Selected
<i>A. trichopoda</i>	lncRNA	5698	4556	4556
	mRNA	26846	22326	4556
<i>A. thaliana</i>	lncRNA	2540	2540	2540
	mRNA	13973	13973	2540
<i>C. sinensis</i>	lncRNA	2562	2215	2215
	mRNA	46147	45846	2215
<i>C. sativus</i>	lncRNA	1929	1730	1730
	mRNA	30364	29829	1730
<i>R. communis</i>	lncRNA	4198	3487	3487
	mRNA	31221	29042	3487

209 The mRNA data of the *Arabidopsis thaliana* (obtained from CPC2 [25])  
210 were built from the RefSeq database with protein sequences annotated by  
211 Swiss-Prot [25], and lncRNA data from the Ensembl (v87) and Ensembl  
212 Plants (v32) database. The mRNA transcript data of the *Amborella tri-*  
213 *chopoda*, *Citrus sinensis*, *Cucumis sativus* and *Ricinus communis* were ex-  
214 tracted from Phytozome (version 13) [75]. The lncRNAs data from these  
215 species were extracted from GreenC (version 1.12) [76].

### 216 3.1.2. Case Study II

217 In this case study, we will apply the best mathematical models (con-  
218 sidering accuracy) of case study I to different classification problems with  
219 lncRNAs, in order to test their generalization. Thus, divided this part into  
220 three problems:

221 • **Problem 1** (lncRNA vs. sncRNA): Dataset with only non-coding  
222 sequences (lncRNA and Small non-coding RNAs (sncRNAs), also ob-  
223 tained from [25])

224 – lncRNA: 1291 sequences — sncRNA: 1291 sequences

225 • **Problem 2** (lncRNA vs. Antisense): Dataset with lncRNAs and long  
226 noncoding antisense transcripts (obtained from [77]).

227 – lncRNA: 57 sequences — Antisense: 57 sequences

228 • **Problem 3** (circRNA vs. lncRNA): Dataset with lncRNA and circu-  
229 lar RNAs (cirRNAs) sequences (circRNA obtained from PlantcircBase  
230 [78]. This problem was based on [21] and [27], in order to classify  
231 circRNA from other lncRNAs.

232 – circRNA: 2540 sequences — lncRNA: 2540 sequences

233 It is important to emphasize that we used only sequences from *Arabidop-*  
234 *sis thaliana* in this second case study because it is the model species in  
235 plants. Moreover, plant sequences is the least addressed field by the studies,  
236 consequently presenting more challenges.

### 237 3.2. Feature Extraction

238 In this section, 9 feature extraction approaches are shown: 6 numer-  
239 ical mapping techniques with Fourier transform, Entropy, Complex Net-  
240 works. It is necessary to emphasize that we denote a biological sequence  
241  $\mathbf{s} = (s[0], s[1], \dots, s[N - 1])$  such that  $\mathbf{s} \in \{A, C, G, T\}^N$  [20].

### 242 3.3. Fourier Transform and Numerical Mappings

243 To extract features based on a Fourier model, we applied the Discrete  
244 Fourier Transform (DFT), widely used for digital image and signal processing  
245 (here GSP), which can reveal hidden periodicities after transformation of  
246 time domain data to frequency domain space [79]. According to Yin and

247 Yau [80], the DFT of a signal with length  $N$ ,  $\mathbf{x} \in \mathbb{R}^N$ , at frequency  $k$ , can  
 248 be defined by Equation (1):

$$X[k] = \sum_{n=0}^{N-1} x[n] e^{-j\frac{2\pi}{N}kn}, \quad k = 0, 1, \dots, N - 1. \quad (1)$$

249 This method is has been widely studied in bioinformatics, mainly for  
 250 analysis of periodicities and repetitive elements in DNA sequences [81] and  
 251 protein structures [82]. This approach is shown in Figure 3 and was based  
 252 on [20].

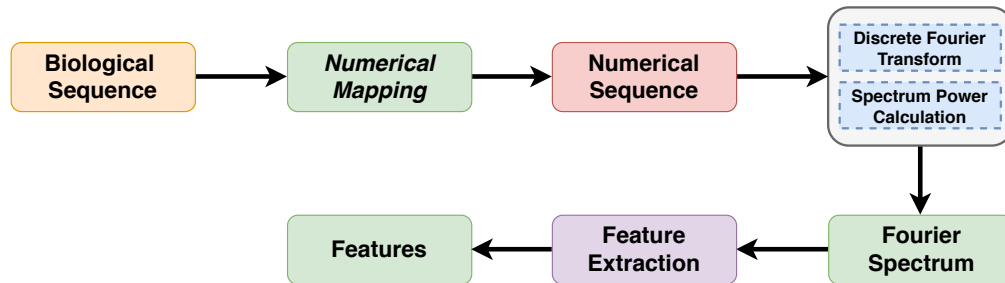


Figure 3: Fourier Transform and Numerical Mapping Pipeline. (1) Each sequence is mapped to a numerical sequence; (2) DFT is applied to the generated sequence; (3) The spectrum power is calculated; (4) The Feature Extraction is performed; Finally, (5) the features are generated.

253 To calculate DFT, we will use the Fast Fourier Transform (FFT), that  
 254 is a highly efficient procedure for computing the DFT of a time series [83].  
 255 However, to use GSP techniques, a numeric representation should be used  
 256 for the transformation or mapping of genomic data. In the literature, distinct  
 257 DNR techniques have been developed [84]. According to Mendizabal-  
 258 Ruiz et al. [85], these representations can be divided into three categories:  
 259 single-value mapping, multidimensional sequence mapping, and cumulative  
 260 sequence mapping. Thereby, we study 6 numerical mapping techniques (or  
 261 representations), which will be presented below: Voss [86], Integer [85, 87],  
 262 Real [88], Z-curve [89], EIIP [90] and Complex Numbers [84, 91, 92].

### 263 3.3.1. Voss Representation

264 This representation can use single or multidimensional vectors. Funda-  
 265 mentally, this approach transforms a sequence  $\mathbf{s} \in \{A, C, G, T\}^N$  into a

266 matrix  $\mathbf{V} \in \{0, 1\}^{4 \times N}$  such that  $\mathbf{V} = [\mathbf{v}_1, \mathbf{v}_2, \mathbf{v}_3, \mathbf{v}_4]^T$ , where  $T$  is the trans-  
 267 pose operator and each  $\mathbf{v}_i$  array is constructed according to the following  
 268 relation:

$$v_i[n] = \begin{cases} 1, & s[n] = \alpha[i] \\ 0, & s[n] \neq \alpha[i] \end{cases}, \quad \text{where } \alpha = (A, C, G, T), \quad n = 0, 1, \dots, N - 1. \quad (2)$$

269 As a result, each row of matrix  $\mathbf{V}$  may be seen as an array that marks each  
 270 base position such that the first row denotes the presence of base  $A$ , row two  
 271 for base  $C$ , row three base  $G$  and the last row for base  $T$ . For example, let  $\mathbf{s} =$   
 272  $(G, A, G, A, G, T, G, A, C, C, A)$  be a sequence that needs to be represented  
 273 using Voss representation, therefore,  $\mathbf{v}_1 = (0, 1, 0, 1, 0, 0, 0, 1, 0, 0, 1)$ , which  
 274 represents the locations of bases  $A$ ,  $\mathbf{v}_2 = (0, 0, 0, 0, 0, 0, 0, 0, 1, 1, 0)$  for bases  
 275  $C$ ,  $\mathbf{v}_3 = (1, 0, 1, 0, 1, 0, 1, 0, 0, 0, 0)$  for the  $G$  bases,  $\mathbf{v}_4 = (0, 0, 0, 0, 0, 1, 0,$   
 276  $0, 0, 0, 0)$  for  $T$  bases. Then, using the DFT in the indicator sequences shown  
 277 above, we obtain (see Equation 3):

$$V_i[k] = \sum_{n=0}^{N-1} v_i[n] e^{-j \frac{2\pi}{N} kn}, \quad \forall i \in [1, 4], \quad k = 0, 1, \dots, N - 1. \quad (3)$$

278 The power spectrum of a biological sequence can be obtained by Equation  
 279 (4):

$$P_V[k] = \sum_{i=1}^4 |V_i[k]|^2, \quad k = 0, 1, \dots, N - 1. \quad (4)$$

### 280 3.3.2. Integer Representation

281 This representation is one-dimensional [87, 85]. This mapping can be  
 282 obtained by substituting the four nucleotides (T, C, A, G) of a biological  
 283 sequence for integers (0, 1, 2, 3), respectively, e.g., let  $\mathbf{s} = (G, A, G, A, G,$   
 284  $T, G, A, C, C, A)$ , thus,  $\mathbf{d} = (3, 2, 3, 2, 3, 0, 3, 2, 1, 1, 2)$ , as exposed in  
 285 Equation (5). The DFT and power spectrum are presented in Equation (6).

$$d[n] = \begin{cases} 3, & s[n] = G \\ 2, & s[n] = A \\ 1, & s[n] = C \\ 0, & s[n] = T \end{cases}, \quad n = 0, 1, \dots, N - 1. \quad (5)$$

$$D[k] = \sum_{n=0}^{N-1} d[n]e^{-j\frac{2\pi}{N}kn}, \quad P_D[k] = |D[k]|^2, \quad k = 0, 1, \dots, N-1. \quad (6)$$

### 286 3.3.3. Real Representation

287 In this representation, Chakravarthy et al. [88] use real mapping based on  
 288 the complement property of the complex mapping of [81]. This mapping ap-  
 289 plies negative decimal values for the purines ( $A, G$ ), and positive decimal val-  
 290 ues for the pyrimidines ( $C, T$ ), e.g., let  $\mathbf{s} = (G, A, G, A, G, T, G, A, C, C, A)$ ,  
 291 thus,  $\mathbf{r} = (-0.5, -1.5, -0.5, -1.5, -0.5, 1.5, -0.5, -1.5, 0.5, 0.5, -1.5)$ , as Equation  
 292 (7) and Equation (8).

$$r[n] = \begin{cases} -0.5, & s[n] = G \\ -1.5, & s[n] = A \\ 0.5, & s[n] = C \\ 1.5, & s[n] = T \end{cases} \quad n = 0, 1, \dots, N-1. \quad (7)$$

293

$$R[k] = \sum_{n=0}^{N-1} r[n]e^{-j\frac{2\pi}{N}kn}, \quad P_R[k] = |R[k]|^2, \quad k = 0, 1, \dots, N-1. \quad (8)$$

### 294 3.3.4. Z-curve Representation

295 The Z-curve scheme is a three-dimensional curve presented by [89], to  
 296 encode DNA sequences with more biological semantics. Essentially, we can  
 297 inspect a given sequence  $s[n]$  of length  $N$ , taking into account the  $n$ -th el-  
 298 ement of the sequence ( $n = 1, 2, \dots, N$ ). Then, we denote the cumulative  
 299 occurrence numbers  $A_n, C_n, G_n$  and  $T_n$  for each base  $A, C, G$  and  $T$ , as the  
 300 number of times that a base occurred from  $s[1]$  up until  $s[n]$ . Fundamentally,  
 301 this method reduces the number of indicator sequences from four (Voss) to  
 302 three (Z-curve) in a symmetrical way for all four components [93]. Therefore:

$$A_n + C_n + G_n + T_n = n \quad (9)$$

303 Where the Z-curve consists of a series of nodes  $P_1, P_2, \dots, P_N$ , whose  
 304 coordinates  $x[n], y[n]$ , and  $z[n]$  ( $n = 1, 2, \dots, N$ ) are uniquely determined by  
 305 the Z-transform, shown in Equation (10):

$$P[n] = \begin{cases} x[n] = (A_n + G_n) - (C_n + T_n) \\ y[n] = (A_n + C_n) - (G_n + T_n), \\ z[n] = (A_n + T_n) - (C_n + G_n) \end{cases} \quad (10)$$

$$x[n], y[n], z[n] \in [-n, n], \quad n = 1, 2, \dots, N.$$

306 The coordinates  $x[n]$ ,  $y[n]$ , and  $z[n]$  represent three independent distri-  
 307 butions that fully describe a sequence [84]. Therefore, we will have three distri-  
 308 butions with definite biological significance: (1)  $x[n]$  = purine/pyrimidine,  
 309 (2)  $y[n]$  = amino/keto, (3)  $z[n]$  = weak hydrogen bonds/strong hydro-  
 310 gen bonds [89], e.g., let  $\mathbf{s} = (G, A, G, A, G, T, G, A, C, C, A)$ , thus,  
 311  $\mathbf{x} = (1, 2, 3, 4, 5, 4, 5, 6, 5, 4, 5)$ ;  $\mathbf{y} = (-1, 0, -1, 0, -1, -2, -3, -2, -1, 0, 1)$ ;  
 312  $\mathbf{z} = (-1, 0, -1, 0, -1, 0, -1, 0, -1, -2, -1)$ . Essentially, the difference be-  
 313 tween each dimension at the  $n$ -th position and the previous  $(n - 1)$  position  
 314 can be either 1 or  $-1$  [89]. Therefore, we may define the following set of  
 315 equations in order to update the values of each dimension array considering  
 316 that  $x[-1] = y[-1] = z[-1] = 0$ :

$$x[n] = \begin{cases} x[n-1] + 1, & s[n] = A \text{ or } G \\ x[n-1] - 1, & s[n] = C \text{ or } T \end{cases} \quad (11)$$

$$y[n] = \begin{cases} y[n-1] + 1, & s[n] = A \text{ or } C \\ y[n-1] - 1, & s[n] = G \text{ or } T \end{cases} \quad n = 1, 2, \dots, N. \quad (12)$$

$$z[n] = \begin{cases} z[n-1] + 1, & s[n] = A \text{ or } T \\ z[n-1] - 1, & s[n] = G \text{ or } C \end{cases} \quad (13)$$

317 Finally, the DFT and power spectrum may be defined as [94]:

$$X[k] = \sum_{n=1}^N x[n]e^{-j\frac{2\pi}{N}kn}, \quad Y[k] = \sum_{n=1}^N y[n]e^{-j\frac{2\pi}{N}kn}, \quad Z[k] = \sum_{n=1}^N z[n]e^{-j\frac{2\pi}{N}kn}. \quad (14)$$

$$P_C[k] = |X[k]|^2 + |Y[k]|^2 + |Z[k]|^2, \quad k = 1, 2, \dots, N. \quad (15)$$

### 318 3.3.5. EIIP Representation

319 Nair and Sreenadhan [90] proposed EIIP values of nucleotides to repre-  
 320 sent biological sequences and to locate exons. According to the authors, a

321 numerical sequence representing the distribution of free electron energies can  
 322 be called "EIIP indicator sequence", e.g., let  $\mathbf{s} = (G, A, G, A, G, T, G, A,$   
 323  $C, C, A)$ , thus,  $\mathbf{b} = (0.0806, 0.1260, 0.0806, 0.1260, 0.0806, 0.1335, 0.0806,$   
 324  $0.1260, 0.1340, 0.1340, 0.1260)$ , as shown in Equation (16). The DFT and  
 325 power spectrum of this representation are presented in Equation (17).

$$b[n] = \begin{cases} 0.0806, & s[n] = G \\ 0.1260, & s[n] = A \\ 0.1340, & s[n] = C' \\ 0.1335, & s[n] = T \end{cases} \quad n = 0, 1, \dots, N - 1. \quad (16)$$

$$B[k] = \sum_{n=0}^{N-1} b[n]e^{-j\frac{2\pi}{N}kn}, \quad P_B[k] = |B[k]|^2, \quad k = 0, 1, \dots, N - 1. \quad (17)$$

### 326 3.3.6. Complex Numbers Representation

327 This numerical mapping has the advantage of better translating some of  
 328 the nucleotides features into mathematical properties [92] and represents the  
 329 complementary nature of AT and CG pairs [84]; e.g., let  $\mathbf{s} = (G, A, G, A,$   
 330  $G, T, G, A, C, C, A)$ , thus,  $\bar{\mathbf{r}} = (-1 - j, 1 + j, -1 - j, 1 + j, -1 - j, 1 - j,$   
 331  $-1 - j, 1 + j, -1 + j, -1 + j, 1 + j)$ , as shown in Equation (18). The DFT  
 332 and power spectrum of this representation are presented in Equation (19).

$$\bar{r}[n] = \begin{cases} -1 - j, & s[n] = G \\ 1 + j, & s[n] = A \\ -1 + j, & s[n] = C' \\ 1 - j, & s[n] = T \end{cases} \quad n = 0, 1, \dots, N - 1. \quad (18)$$

$$\bar{R}[k] = \sum_{n=0}^{N-1} \bar{r}[n]e^{-j\frac{2\pi}{N}kn}, \quad P_{\bar{R}}[k] = |\bar{R}[k]|^2, \quad k = 0, 1, \dots, N - 1. \quad (19)$$

### 333 3.3.7. Features

334 The feature extraction is applied in each representation with Fourier  
 335 transform, adopting Peak to Average Power Ratio (PAPR), mistakenly con-  
 336 fused with the Signal to Noise Ratio (SNR), average power spectrum, me-  
 337 dian, maximum, minimum, sample standard deviation, population standard  
 338 deviation, percentile (15/25/50/75), amplitude, variance, interquartile range,

339 semi-interquartile range, coefficient of variation, skewness, and kurtosis. Ac-  
 340 cording to [95], the RNA has a statistical phenomenon known as period-3  
 341 behavior or 3-base periodicity, where the peak power will always be at the  
 342 sample  $N/3$ . The PAPR is defined as [96]:

$$PAPR = \frac{\max_{0 \leq k \leq N-1} (P[k])}{\frac{1}{N} \sum_{k=0}^{N-1} P[k]} \quad (20)$$

### 343 3.4. Entropy

344 Information theory has been widely used in bioinformatics [97, 98]. Based  
 345 on this, we consider the study of [99], which applied an algorithmic and  
 346 mathematical approach to DNA code analysis using entropy and phase plane.  
 347 According to [98], entropy is a measure of the uncertainty associated with a  
 348 probabilistic experiment. To generate a probabilistic experiment, we use a  
 349 known approach in bioinformatics, the k-mer (our pipeline - Figure 4).

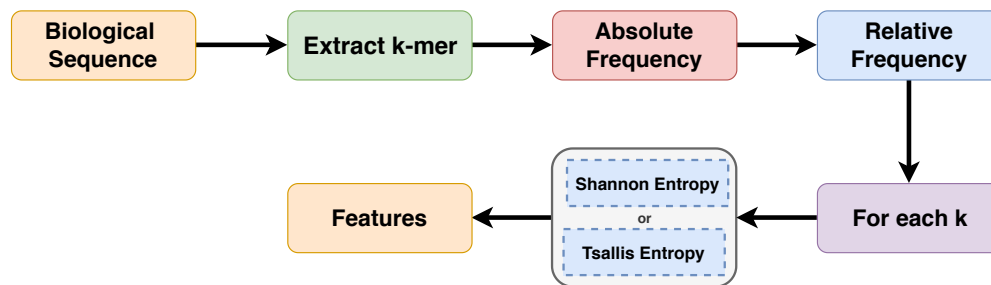


Figure 4: Entropy Pipeline. (1) Each sequence is mapped in  $k$ -mers; (2) The absolute frequency of each  $k$  is calculated; (3) Based on absolute frequency, the relative frequency is calculated; (4) The Tsallis or Shannon entropy is applied to each  $k$ .

350 In this method, each sequence is mapped in the frequency of neighboring  
 351 bases  $k$ , generating statistical information. The  $k$ -mer is denoted by  $P_k$ ,  
 352 corresponding to Equation (21).

$$P_k(\mathbf{s}) = \frac{c_i^k}{N - k + 1} = \left( \frac{c_1^1}{N - 1 + 1}, \dots, \frac{c_4^1}{N - 1 + 1}, \right. \\ \left. \frac{c_{4+1}^2}{N - 2 + 1}, \dots, \frac{c_i^k}{N - k + 1} \right) \quad k = 1, 2, \dots, 24. \quad (21)$$



353 We applied this equation to each sequence with frequencies of  $k = 1, 2,$   
 354  $\dots, 24$ . Where,  $c_i^k$  is the number of substring occurrences with length  $k$  in a  
 355 sequence ( $\mathbf{s}$ ) with length  $N$ , in which the index  $i \in \{1, 2, \dots, 4^1 + \dots + 4^k\}$   
 356 represents the analyzed substring. For a better understanding, Figure 5  
 357 demonstrated an example with  $k = 6$  and  $k = 9$ .

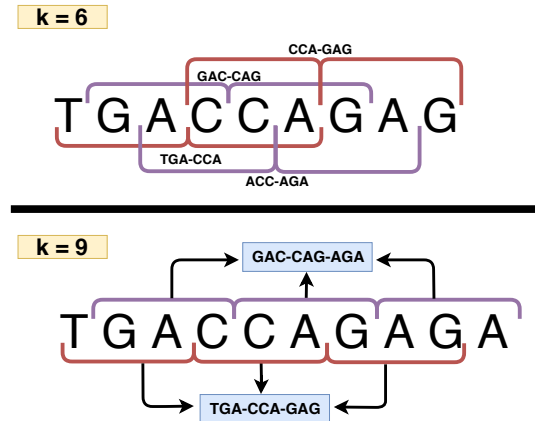


Figure 5:  $k$ -mer Workflow. Example with  $k = 6$  and  $k = 9$ .

358 Basically, histograms with short bins are adopted, such as  $\{\{A\}, \{C\},$   
 359  $\{G\}, \{T\}\}$ , that occur for  $k = 1$ , up to histograms with long sequence counting  
 360 bins such as  $\{\{GGGGGGGGGGGG\}, \dots, \{AAAAAAAAAAAAA}\}$ , that  
 361 result for  $k = 12$ . Where, after counting the absolute frequencies of each  $k$ ,  
 362 we generate relative frequencies (see Equation (21)), and then apply Shannon  
 363 and Tsallis entropy to generate the features.

### 3.4.1. Shannon and Tsallis Entropy

365 Fundamentally, we chose Shannon entropy, because it quantifies the amount  
 366 of information in a variable [100], that is, we can reach a single value that  
 367 quantifies the information contained in different observation periods (e.g.,  
 368 our case:  $k$ -mer). However, according to [101], it is important to explore a  
 369 generalized form of the Shannon's entropy. Based on this, we have opted for  
 370 a generalized entropy proposed by Tsallis, applied by several works in the lit-  
 371 erature [102, 103]. Thereby, for a discrete random variable  $F$  taking values in  
 372  $\{f[0], f[1], f[2], \dots, f[N-1]\}$  with probabilities  $\{p[0], p[1], p[2], \dots, p[N-1]\}$ ,  
 373 represented as  $P(F = f[n]) = p[n]$ . The Shannon (Equation 22) and Tsallis  
 374 (Equation 23) entropy associated with this variable is given by the following  
 375 expressions:

$$H_S[k] = - \sum_{n=0}^{N-1} p_k[n] \log_2 p_k[n] \quad k = 1, 2, \dots, 24. \quad (22)$$

$$H_T[k] = \frac{1}{q-1} \left( 1 - \sum_{n=0}^{N-1} p_k[n]^q \right) \quad k = 1, 2, \dots, 24. \quad (23)$$

376 Where  $k$  represents the analyzed  $k$ -mer,  $N$  the number of possible events  
 377 and  $p[n]$  the probability that event  $n$  occurs.

### 378 3.5. Complex Networks

379 Complex networks are widely used in mathematical modeling and have  
 380 been an extremely active field in recent years [104], as well as becoming an  
 381 ideal research area for mathematicians, computer scientists, and biologists.  
 382 Based on this, we consider the study of [66], in which we propose a feature  
 383 extraction model based on complex networks, as shown in Figure 6.

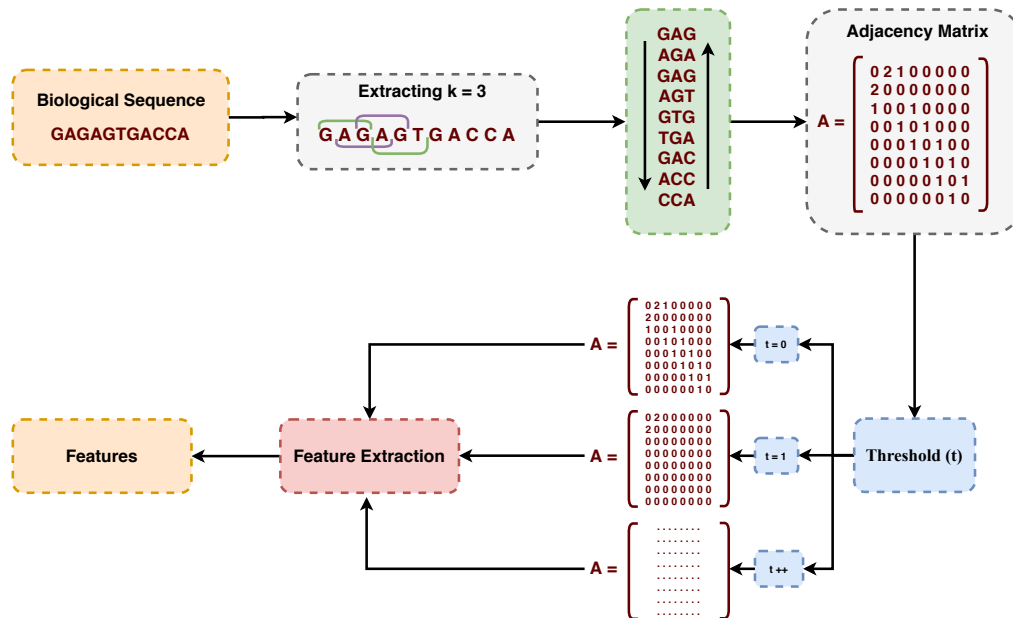


Figure 6: Complex Networks Pipeline. (1) Each sequence is mapped in the frequency of neighboring bases  $k$  ( $k = 3$ ); (2) This mapping is converted to a undirected graph represented by an adjacency matrix; (3) Feature extraction is performed using a threshold scheme; Finally, (4) the features are generated.

384 Each sequence is mapped to the frequency of neighboring bases  $k$  ( $k =$   
385  $3$  - see Figure 5). This mapping is converted into an undirected graph rep-  
386 resented by an adjacency matrix, in which we applied a threshold scheme  
387 for feature extraction, thus generating our characteristic vector. Fundamen-  
388 tally, we represent our structure by undirected weighted graphs. According  
389 to [104], a graph  $G = \{V, E\}$  is structured by a set  $V$  of vertices (or nodes)  
390 connected by a set  $E$  of edges (or links). Each edge reflects a link between  
391 two vertices, e.g.,  $e_p = (i, j)$  connection between the vertices  $i$  and  $j$  [104].  
392 If there is an edge connecting the vertices  $i$  and  $j$ , the elements  $a_{ij}$  are equal  
393 to 1, and equal to 0 otherwise.

394 In our case, the graph is undirected, that is, the adjacency matrix  $A$   
395 is symmetric, e.g., elements  $a_{ij} = a_{ji}$  for any  $i$  and  $j$  [104]. Furthermore,  
396 we apply a threshold scheme presented by [66], in which we extract weight  
397 of the edges to capture adjacencies at different frequencies. Finally, as fea-  
398 tures, several network characterization measures were obtained, based on  
399 [66, 105], among them: Betweenness, assortativity, average degree, average  
400 path length, minimum degree, maximum degree, degree standard deviation,  
401 frequency of motifs (size 3 and 4), clustering coefficient.

### 402 *3.6. Normalization, Training and Evaluation Metrics*

403 Data normalization is a preprocessing technique often applied to a dataset.  
404 Essentially, features can have different dynamic ranges. This problem may  
405 have a stronger effect in the induction of a predictive model, mainly for  
406 distance-based ML algorithms. Consequently, the application of a normal-  
407 ization procedure makes the ranges similar, reducing this problem [106]. We  
408 used the min-max normalization, which reduces the data range to 0 and 1  
409 (or -1 to 1, if there are negative values) [20]. The general formula is given as  
410 (Equation (24)) [107]:

$$x'_{ij} = \frac{x_{ij} - \min(j)}{\max(j) - \min(j)}. \quad (24)$$

411 Where  $x$  is the original value and  $x'_{ij}$  is its normalized version. Further-  
412 more,  $\min(j)$  and  $\max(j)$  are, respectively, the smallest and largest values of  
413 a feature  $j$  [6, 107]. Next, we investigate three classification algorithms, such  
414 as Random Forest (RF) [108], AdaBoost [109] and CatBoost [110]. We chose  
415 these ML algorithms because they induce interpretable predictive models  
416 when humans can easily understand the internal decision-making process.  
417 Thus, domain experts can validate the knowledge used by the models for

418 the classification of new sequences [6]. Finally, to induce our models, we  
419 used 70% of samples for *training* (with 10-fold cross-validation) and 30% for  
420 *testing*, as shown in Table 2.

Table 2: Number of sequences used for training and testing in each dataset.

Case Study	Dataset	Samples	Training	Testing
<b>I</b>	<i>A. trichopoda</i>	9112	6378	2734
	<i>A. thaliana</i>	5080	3556	1524
	<i>C. sinensis</i>	4430	3101	1329
	<i>C. sativus</i>	3460	2422	1038
	<i>R. communis</i>	6974	4881	2093
<b>II</b>	<i>lncRNA vs. sncRNA</i>	2582	1807	775
	<i>lncRNA vs. Antisense</i>	114	79	35
	<i>circRNA vs. lncRNA</i>	5080	3556	1524

421 The methods were evaluated with four measures: Sensitivity (SE - Equa-  
422 tion 26), Specificity (SPC - Equation 27), Accuracy (ACC - Equation 25),  
423 and Cohen’s kappa coefficient [111] (Equation 28).

$$ACC = \frac{TP + TN}{TN + FP + TP + FN} \quad SPC = \frac{TN}{TN + FP} \quad (27)$$

$$SE = \frac{TP}{TP + FN} \quad (26) \quad Kappa = \frac{p_o - p_e}{1 - p_e} \quad (28)$$

424 These measures use True Positive (TP), True Negative (TN), False Posi-  
425 tive (FP) and False Negative (FN) values, where: TP measures the correctly  
426 predicted positive label; TN represents the correctly classified negative label;  
427 FP describes all those negative entities that are incorrectly classified as posi-  
428 tive and; FN represents the positive label that are incorrectly classified as  
429 the negative label.

#### 430 4. Results

431 This section shows experimental results from 9 feature extraction ap-  
432 proaches with mathematical models for biological sequences, divided into  
433 two parts: Case Study I and Case Study II.

434 *4.1. Case Study I*

435 Initially, we induced models with the RF, AdaBoost, and CatBoost clas-  
 436 sifiers in the training set of three datasets (*A. trichopoda*, *A. thaliana*, and *R.*  
 437 *communis*, we randomly chose three datasets for evaluating the classifiers).  
 438 Our initial goal is to choose the best classifier to follow in the testing phases.  
 439 Thereby, to estimate the real accuracy, we applied 10-fold cross-validation,  
 440 as shown in Table 3.

Table 3: Accuracy for the training set (*A. trichopoda*, *A. thaliana*, and *R. communis*) using 10-fold cross-validation.

Dataset	Model	RF	AdaBoost	CatBoost
<i>A. trichopoda</i>	Z-curve	0.90 ( $\pm$ 0.03)	0.91 ( $\pm$ 0.02)	<b>0.92 (<math>\pm</math> 0.02)</b>
	Binary	0.92 ( $\pm$ 0.02)	<b>0.94 (<math>\pm</math> 0.02)</b>	<b>0.94 (<math>\pm</math> 0.02)</b>
	Real	0.91 ( $\pm$ 0.02)	0.93 ( $\pm$ 0.02)	<b>0.94 (<math>\pm</math> 0.02)</b>
	Integer	0.91 ( $\pm$ 0.02)	0.93 ( $\pm$ 0.02)	<b>0.94 (<math>\pm</math> 0.02)</b>
	EIIP	0.92 ( $\pm$ 0.02)	<b>0.94 (<math>\pm</math> 0.02)</b>	<b>0.94 (<math>\pm</math> 0.02)</b>
	Complex	0.92 ( $\pm$ 0.03)	<b>0.94 (<math>\pm</math> 0.02)</b>	<b>0.94 (<math>\pm</math> 0.02)</b>
	Graphs	0.92 ( $\pm$ 0.02)	<b>0.94 (<math>\pm</math> 0.02)</b>	<b>0.94 (<math>\pm</math> 0.02)</b>
	Shannon	0.92 ( $\pm$ 0.02)	<b>0.94 (<math>\pm</math> 0.02)</b>	<b>0.94 (<math>\pm</math> 0.02)</b>
	Tsallis	0.92 ( $\pm$ 0.02)	<b>0.94 (<math>\pm</math> 0.02)</b>	<b>0.94 (<math>\pm</math> 0.02)</b>
<i>A. thaliana</i>	Z-curve	<b>0.95 (<math>\pm</math> 0.02)</b>	0.93 ( $\pm$ 0.03)	0.94 ( $\pm$ 0.02)
	Binary	<b>0.94 (<math>\pm</math> 0.02)</b>	<b>0.94 (<math>\pm</math> 0.02)</b>	<b>0.94 (<math>\pm</math> 0.02)</b>
	Real	<b>0.95 (<math>\pm</math> 0.02)</b>	0.94 ( $\pm$ 0.02)	<b>0.95 (<math>\pm</math> 0.02)</b>
	Integer	<b>0.94 (<math>\pm</math> 0.02)</b>	<b>0.94 (<math>\pm</math> 0.02)</b>	<b>0.94 (<math>\pm</math> 0.02)</b>
	EIIP	<b>0.95 (<math>\pm</math> 0.02)</b>	0.94 ( $\pm$ 0.02)	0.95 ( $\pm$ 0.03)
	Complex	0.94 ( $\pm$ 0.02)	0.94 ( $\pm$ 0.02)	<b>0.94 (<math>\pm</math> 0.01)</b>
	Graphs	0.94 ( $\pm$ 0.02)	0.94 ( $\pm$ 0.02)	<b>0.95 (<math>\pm</math> 0.02)</b>
	Shannon	0.94 ( $\pm$ 0.02)	0.94 ( $\pm$ 0.02)	<b>0.95 (<math>\pm</math> 0.02)</b>
	Tsallis	<b>0.94 (<math>\pm</math> 0.02)</b>	<b>0.94 (<math>\pm</math> 0.02)</b>	<b>0.94 (<math>\pm</math> 0.02)</b>
<i>R. communis</i>	Z-curve	<b>0.93 (<math>\pm</math> 0.02)</b>	0.92 ( $\pm$ 0.02)	<b>0.93 (<math>\pm</math> 0.02)</b>
	Binary	<b>0.95 (<math>\pm</math> 0.01)</b>	0.95 ( $\pm$ 0.02)	0.95 ( $\pm$ 0.02)
	Real	<b>0.95 (<math>\pm</math> 0.02)</b>	0.94 ( $\pm$ 0.02)	0.94 ( $\pm$ 0.02)
	Integer	<b>0.94 (<math>\pm</math> 0.01)</b>	<b>0.94 (<math>\pm</math> 0.01)</b>	0.94 ( $\pm$ 0.02)
	EIIP	0.95 ( $\pm$ 0.02)	0.95 ( $\pm$ 0.02)	<b>0.95 (<math>\pm</math> 0.01)</b>
	Complex	0.95 ( $\pm$ 0.02)	<b>0.95 (<math>\pm</math> 0.01)</b>	<b>0.95 (<math>\pm</math> 0.01)</b>
	Graphs	<b>0.95 (<math>\pm</math> 0.01)</b>	<b>0.95 (<math>\pm</math> 0.01)</b>	0.95 ( $\pm$ 0.02)
	Shannon	0.95 ( $\pm$ 0.02)	0.95 ( $\pm$ 0.02)	<b>0.95 (<math>\pm</math> 0.01)</b>

Tsallis	<b>0.95 (<math>\pm</math> 0.01)</b>	<b>0.95 (<math>\pm</math> 0.01)</b>	<b>0.95 (<math>\pm</math> 0.01)</b>
---------	-------------------------------------	-------------------------------------	-------------------------------------

441 Assessing each classifier, we noted that the best performance was of the  
 442 CatBoost with all mathematical models in *A. trichopoda*, followed by Ad-  
 443 aBoost (6 best results) and RF (no better results). In *A. thaliana*, CatBoost  
 444 kept the best performance (7 best results), followed by RF (6 best results)  
 445 and AdaBoost (3 best results). In contrast, the RF classifier obtained the  
 446 best results (6) in *R. communis*, followed by CatBoost (5 best results) and  
 447 AdaBoost (3 best results). Based on this, we continued testing the models  
 448 with the CatBoost classifier. Thus, in Table 4, we present the results of all  
 449 mathematical models using 4 evaluation metrics.

Table 4: Performance analysis. This table compares the sensitivity, specificity, accuracy and kappa metrics for each model in the test sets using CatBoost classifier.

Dataset	Model	SE	SPC	ACC	Kappa
<i>A. trichopoda</i>	Z-curve	0.9744	0.8566	0.9155	0.8310
	Binary	0.9795	0.9005	0.9400	0.8800
	Real	<b>0.9802</b>	0.8837	0.9320	0.8639
	Integer	0.9773	0.8822	0.9298	0.8595
	EIIP	0.9781	0.8990	0.9386	0.8771
	Complex	<b>0.9802</b>	0.9012	<b>0.9407</b>	<b>0.8815</b>
	Graphs	0.9737	<b>0.9020</b>	0.9378	0.8756
	Shannon	0.9781	<b>0.9020</b>	0.9400	0.8800
	Tsallis	0.9795	0.9005	0.9400	0.8800
	<i>A. thaliana</i>	Z-curve	0.9777	0.9383	0.9580
Binary		0.9619	0.9449	0.9534	0.9068
Real		<b>0.9803</b>	0.9409	<b>0.9606</b>	<b>0.9213</b>
Integer		0.9698	0.9436	0.9567	0.9134
EIIP		0.9646	0.9449	0.9547	0.9094
Complex		0.9724	0.9409	0.9567	0.9134
Graphs		0.9685	0.9423	0.9554	0.9108
Shannon		0.9738	<b>0.9462</b>	0.9600	0.9200
Tsallis		0.9764	0.9409	0.9587	0.9173
		Z-curve	0.9021	<b>0.8707</b>	0.8864
	Binary	0.8901	<b>0.8707</b>	0.8804	0.7607
	Real	0.9142	0.8571	0.8856	0.7713

<i>C. sinensis</i>	Integer	0.8825	0.8692	0.8758	0.7517
	EIIP	0.8840	0.8526	0.8683	0.7367
	Complex	0.9081	0.8496	0.8789	0.7577
	Graphs	0.9006	0.8632	0.8819	0.7637
	Shannon	0.9172	0.8586	0.8879	0.7758
	Tsallis	<b>0.9262</b>	0.8541	<b>0.8901</b>	<b>0.7803</b>
<i>C. sativus</i>	Z-curve	0.8979	0.8478	0.8728	0.7457
	Binary	0.9056	0.8459	0.8757	0.7514
	Real	0.9268	0.8439	0.8854	0.7707
	Integer	0.9056	<b>0.8536</b>	0.8796	0.7592
	EIIP	0.8979	0.8459	0.8719	0.7437
	Complex	0.9326	0.8343	0.8834	0.7669
	Graphs	0.9075	<b>0.8536</b>	0.8805	0.7611
	Shannon	0.9326	0.8382	0.8854	0.7707
	Tsallis	<b>0.9403</b>	0.8401	<b>0.8902</b>	<b>0.7803</b>
<i>R. communis</i>	Z-curve	0.9446	0.9140	0.9293	0.8586
	Binary	0.9417	0.9589	0.9503	0.9006
	Real	<b>0.9589</b>	0.9408	0.9498	0.8997
	Integer	0.9465	0.9456	0.9460	0.8920
	EIIP	0.9455	0.9551	0.9503	0.9006
	Complex	0.9398	0.9561	0.9479	0.8958
	Graphs	0.9455	0.9542	0.9498	0.8997
	Shannon	0.9388	0.9589	0.9489	0.8978
	Tsallis	0.9417	<b>0.9608</b>	<b>0.9513</b>	<b>0.9025</b>

450 As can be seen, all models presented robust results, with the worst per-  
451 formance (ACC) of 0.8901 (*C. sinensis*) and the best of 0.9606 (*A. thaliana*).  
452 That is, all models were robust in different datasets without a high loss of  
453 performance. Assessing each metric individually, we realized that in SE,  
454 the best performance was from Real representation (3 datasets), followed by  
455 Tsallis (2 datasets) and Complex numbers (1 dataset). In SPC, the best  
456 results were from Entropy (3 datasets), followed by Graphs (2 datasets). In  
457 ACC, Tsallis presented the best performance (3 datasets), followed by Real  
458 representation and Complex numbers (1 dataset). For each dataset, we can  
459 see in *A. trichopoda* the best ACC was 0.9407 (Complex); *A. thaliana* with  
460 0.9606 (Real); *C. sinensis* with 0.8901 (Tsallis); *C. sativus* with 0.8902 (Tsal-  
461 lis); and *R. communis* with 0.9513 (Tsallis). Highlight for Tsallis entropy,  
462 which presented the best results, mainly in accuracy, proving to be more

463 generalist in the case study I.

#### 464 4.2. Case Study II

465 After evaluating all methods in 5 datasets (lncRNA of different species)  
466 and observing their results, we applied a second case study, where we used  
467 only three mathematical models for generalization analysis, including GSP  
468 (Fourier + complex numbers), entropy (Tsallis) and graphs (complex net-  
469 works). Here, our objective was to analyze how each model (feature extrac-  
470 tion approach) behaved in different biological sequence classification prob-  
471 lems. In other words, we assessed the generalization of each approach to  
472 classifying sequences with different structures (distinct problem). For this,  
473 we tested 3 new datasets established in Section 3.1.2, as can be seen in Figure  
474 7.

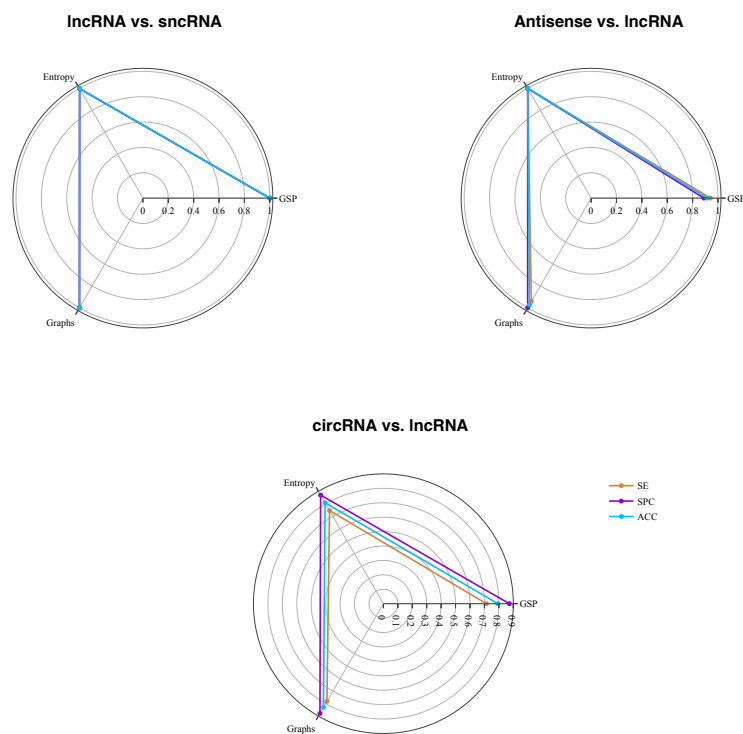


Figure 7: Performance analysis of three mathematical models, GSP (fourier + complex numbers), entropy (Tsallis) and graphs (complex networks), for different problems.



475 Again, all showed robust results, in which, graph-based models are the  
 476 best in 2 of the 3 problems analyzed, followed by entropy and GSP. In the  
 477 three datasets, our approaches have achieved relevant results with ACC, SE  
 478 and SPC, proving to be efficient and generalist, when exposed to different  
 479 problem scenarios. Furthermore, if we analyze at the last problem (circRNA  
 480 vs. lncRNA), our approaches were effective when compared to our references  
 481 that reached an ACC of 0.7780 [21] and 0.7890 [27] in their datasets against  
 482 0.8307 from our best model (graph - using these comparisons as an (indirect)  
 483 reference indicator).

#### 484 4.3. Statistical Significance Tests

485 The statistical significance was assessed in both case studies (difference  
 486 in ACC), using Friedman’s statistical test and the Conover post-hoc test.  
 487 Thereby, our null hypothesis ( $H_0 = M(1) = M(2) = \dots = M(k)$ ), is tested  
 488 against the alternative hypothesis ( $H_A =$  at least one model has statistical  
 489 significance ( $\alpha = 0.05, p < \alpha$ )). First, we apply the global test in the case  
 490 study I, in which the Friedman test indicates significance ( $\chi^2(8) = 17.34, p$ -  
 491 value = 0.0268), that is, we can reject  $H_0$ , as  $p < 0.05$ . Thus, it is essential to  
 492 execute the post-hoc statistical test. Conover statistics values were obtained,  
 493 as well as  $p$ -values (see Table 5), using 95% of significance ( $\alpha = 0.05$ ).

Table 5: Conover statistics values - The accepted alternative hypothesis is in bold ( $p$ -values for  $\alpha = 0.05$ ).

	Z-curve	Binary	Real	Integer	EIIP	Complex	Graphs	Shannon
Binary	0.5580	-	-	-	-	-	-	-
Real	0.1416	0.3671	-	-	-	-	-	-
Integer	0.7896	0.3956	0.0852	-	-	-	-	-
EIIP	0.9574	0.5230	0.1284	0.8309	-	-	-	-
Complex	0.3671	0.7489	0.5580	0.2451	0.3399	-	-	-
Graphs	0.5580	1.0000	0.3671	0.3956	0.5230	0.7489	-	-
Shannon	0.0687	0.2057	0.7089	<b>0.0390</b>	0.0616	0.3399	0.2057	-
Tsallis	<b>0.0146</b>	0.0550	0.2898	<b>0.0075</b>	<b>0.0128</b>	0.1050	0.0550	0.4892

494 Concerning to the Conover post-hoc test, entropy-based models have  
 495 highly significant differences for the Z-curve ( $p < 0.0146$ ), Integer ( $p < 0.0075$   
 496 - Tsallis and  $p < 0.0390$  - Shannon), and EIIP ( $p < 0.0128$ ). Possibly,  
 497 these results indicate that entropy has a more significant performance when  
 498 compared to representations with Fourier. However, other mathematical  
 499 models in case study I do not differ significantly, indicating their efficiency

500 in all datasets. Now, evaluating case study II, we realized that the global  
501 test with Friedman’s statistical test is not significant, in which we obtained  
502  $\chi^2(2) = 1.64$ ,  $p$ -value = 0.4412, indicating that the three studied feature ex-  
503 traction techniques show a similar performance in the problems, once more  
504 confirming the effectiveness and robustness of all mathematical models.

#### 505 4.4. Computational Time

506 In addition, we also assessed the computational time cost of each tested  
507 model. To do this, we ran three models, GSP (Fourier + complex numbers),  
508 entropy (Tsallis) and graphs (complex networks)), in 1291 random sequences,  
509 as shown in Figure 8.

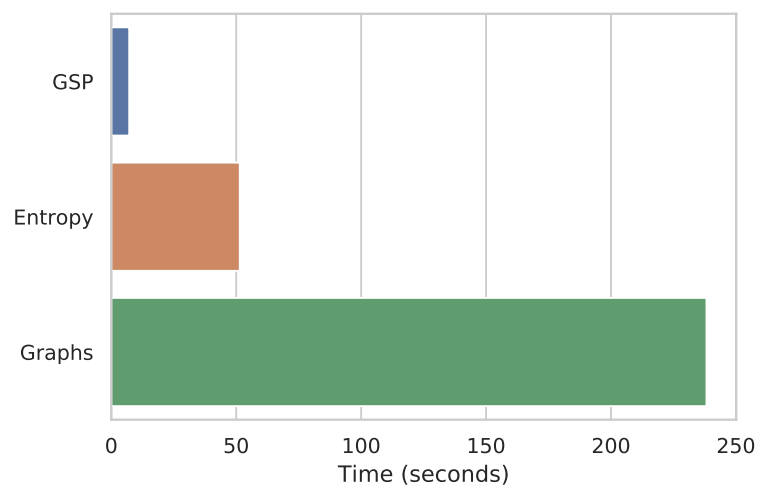


Figure 8: Execution Time.

510 We performed the experiments using Intel Core i3-9100F CPU (3.60GHz),  
511 16GB memory, and running in Debian GNU/Linux 10. The lowest cost in  
512 computational time is for models based on GSP (0m7.183s) and entropy  
513 (0m51.427s), while graphs (3m58.208s) have a much higher cost. These re-  
514 sults demonstrated that, although the models present a similar performance,  
515 the computational time efficiency is significantly different.

## 516 5. Discussion

517 This section discusses our findings in terms of whether they support our  
518 hypothesis (*feature extraction approaches based on mathematical models are*  
519 *as efficient and generalist as biological approaches*). Overall, several exper-  
520 imental tests were assumed in this research, in which all feature extraction  
521 approaches based on mathematical models showed excellent results, as can  
522 be seen in Table 4 and Figure 7. Regarding its performance in distinct clas-  
523 sification problems, case study II, we used only three mathematical models  
524 for generalization analysis, including GSP (Fourier + complex numbers), en-  
525 tropy (Tsallis) and graphs (complex networks). In which, entropy and graph-  
526 based models reported the best performance followed by GSP. Furthermore,  
527 all models maintained robust results in different sequence classification prob-  
528 lems.

529 Furthermore, to fully support our hypothesis, we also compare three  
530 mathematical models shown in Figure 7 concerning a biological and hybrid  
531 approach, in four datasets ((lncRNA vs. mRNA (case study I)); (lncRNA vs.  
532 snRNA; lncRNA vs. Antisense; circRNA vs. lncRNA (case study II)). Thus,  
533 we generate our biological model using some of the most applied features in  
534 Figure 1. Thus, features used by the models are:

- 535 • **Biological:** The features were provided by [25]: Fickett TESTCODE  
536 score, isoelectric point, open reading frame (ORF) length, and ORF  
537 integrity.
- 538 • **Hybrid:** The features were generated by one of the most current ap-  
539 proaches in the literature (lncFinder [26] - 2018). We classify this model  
540 as a hybrid because it uses a combination of biological and mathemati-  
541 cal features. Among the biological characteristics is Logarithm-distance  
542 of hexamer on ORF, length and coverage of the longest ORF. Regard-  
543 ing mathematical features, [26] uses an EIIP-based physicochemical  
544 property with Fourier Transform (similar to our approach with GSP,  
545 but using only EIIP mapping).

546 For a fair comparison, the new experiments follow the same methodology  
547 (70% training, 30% test, and CatBoost classifier), as shown in Table 6.

548 As can be seen, the hybrid model (0.9915) reported the best performance  
549 in the first dataset (lncRNA vs. mRNA), followed by the biological (0.9816)  
550 and our mathematical model (Entropy - 0.9587), with only a difference of

Table 6: Performance analysis of three mathematical models against a biological and hybrid model for different sequence classification problems.

lncRNA vs. mRNA				lncRNA vs. snRNA			
Models	SE	SPC	ACC	Models	SE	SPC	ACC
GSP	0.9724	0.9409	0.9567	GSP	<b>1.0000</b>	<b>1.0000</b>	<b>1.0000</b>
Entropy	<b>0.9764</b>	<b>0.9409</b>	<b>0.9587</b>	Entropy	0.9974	0.9974	0.9974
Graphs	0.9685	0.9423	0.9554	Graphs	<b>1.0000</b>	<b>1.0000</b>	<b>1.0000</b>
Biological	<b>0.9869</b>	<b>0.9764</b>	<b>0.9816</b>	Biological	0.7855	0.8273	0.8065
Hybrid	<b>0.9895</b>	<b>0.9934</b>	<b>0.9915</b>	Hybrid	0.9509	0.9485	0.9497

lncRNA vs. Antisense				circRNA vs. lncRNA			
Models	SE	SPC	ACC	Models	SE	SPC	ACC
GSP	0.9412	0.8889	0.9143	GSP	0.7139	0.8727	0.7933
Entropy	<b>1.0000</b>	<b>1.0000</b>	<b>1.0000</b>	Entropy	0.7467	0.8701	0.8084
Graphs	0.9412	1.0000	0.9714	Graphs	<b>0.7822</b>	<b>0.8793</b>	<b>0.8307</b>
Biological	0.8889	0.9412	0.9143	Biological	0.6024	0.7612	0.6818
Hybrid	0.9412	0.7778	0.8571	Hybrid	0.7283	0.8819	0.8051

551 0.0328 and 0.0229, respectively. However, it is relevant to highlight that  
552 the biological and hybrid models use the ORF descriptor, a highly employed  
553 feature for discovering coding sequences and which, according to [19] is an  
554 essential guideline for distinguishing lncRNAs from mRNA. In other words,  
555 this explains the great result, but, as mentioned at the beginning of this  
556 manuscript, this type of feature with a biological insight is often difficult to  
557 reuse or adapt to another specific problem. Thereby, our study has an gain  
558 in terms of generalization, since this would not be possible only with the  
559 ORF. If we analyze at the hybrid model, in this first dataset, the gain was  
560 minimal compared to the biological (0.0099), confirming the efficiency of the  
561 previously mentioned features (ORF). This is different from our approaches,  
562 which showed an robust result without using bias features for the analyzed  
563 problem.

564 Hence, this hypothesis is proven in the other three datasets, where our  
565 mathematical models perform much better than the biological model, mainly  
566 in the fourth dataset (circRNA vs. lncRNA), in which we obtained a gain  
567 of 0.1489 in ACC. Regarding the hybrid model, it can be observed that the  
568 mixture of biological and mathematical characteristics helped to keep the

569 model competitive in all datasets, indicating the effectiveness of mathemati-  
570 cal features. Even so, our models showed the best results in three of the four  
571 proposed problems. Therefore, our pipeline is efficient in terms of general-  
572 ization to classify lncRNA from mRNA, as well as other biological sequence  
573 classification problems. We also assessed the statistical significance of the  
574 mathematical versus biological approach in the previously applied tests, in  
575 which entropy ( $p < 0.0480$ ) and graphs ( $p < 0.0200$ ) indicated significant re-  
576 sults concerning the biological model. Lastly, considering all these findings,  
577 we fully support the suggested hypothesis.

## 578 6. Conclusion

579 This work proposed to analyze feature extraction approaches for biolog-  
580 ical sequence classification. Specifically, we concentrated our work on the  
581 study of feature extraction techniques using mathematical models. We ana-  
582 lyzed mathematical models to propose efficient and generalist techniques for  
583 different problems. As a case study, we used lncRNA sequences. Moreover,  
584 we divided this paper into two case studies. In our experiments, as a start-  
585 ing point, 9 mathematical models for feature extraction were analyzed: 6  
586 numerical mapping techniques with Fourier transform; Tsallis and Shannon  
587 entropy; Graphs (complex networks). Thereby, several biological sequence  
588 classification problems were adopted to validate the proposed approach.

589 In our experiments, all mathematical models presented relevant and ro-  
590 bust results, with performances (ACC) between 0.8901-0.9606 in case study I.  
591 In case study II, once more, all showed effective results with models based on  
592 entropy and graphs showing the best performance, followed by GSP. Further-  
593 more, to validate our study, we compared three mathematical models against  
594 a biological and hybrid approach, in four different datasets. In which, our  
595 models demonstrated suitable results, and was superior or competitive and  
596 robust in terms of generalization. Moreover, we verified that mathematical  
597 approaches perform as accurately as biological approaches and have a better  
598 generalization capacity since they outperform biological features in scenarios  
599 not designed for them. Finally, among the different feature extraction ap-  
600 proaches tested in this work, the combination of k-mer and entropy, as well  
601 as complex networks performs better than GSP at the cost of a significant  
602 increase in computational complexity.

603 **Declaration of Competing interests**

604 All authors declare that they have no conflict of interest.

605 **Financial support**

606 This project has been supported by a master scholarship from Federal  
607 University of Technology - Paraná (UTFPR) (Grant: April/2018), CAPES  
608 (April/2019 and PROEX-11919694/D), and PROBAL (Grant: CAPES/DAAD  
609 - 88887.144045/2017-00).

610 **Acknowledgements**

611 The authors would like to thank UTFPR-CP, ICMC-USP, and CAPES  
612 for the financial support given to this research.

**References**

- [1] H. Lou, M. Schwartz, J. Bruck, F. Farnoud, Evolution of k-mer frequencies and entropy in duplication and substitution mutation systems, *IEEE Transactions on Information Theory* (2019).
- [2] Y. Li, C. Huang, L. Ding, Z. Li, Y. Pan, X. Gao, Deep learning in bioinformatics: Introduction, application, and perspective in the big data era, *Methods* 166 (2019) 4 – 21, deep Learning in Bioinformatics. doi:<https://doi.org/10.1016/j.ymeth.2019.04.008>.
- [3] R. Min, *Machine Learning Approaches to Biological Sequence and Phenotype Data Analysis*, University of Toronto, 2010.
- [4] M.-R. Cao, Z.-P. Han, J.-M. Liu, Y.-G. Li, Y.-B. Lv, J.-B. Zhou, J.-H. He, Bioinformatic analysis and prediction of the function and regulatory network of long non-coding rnas in hepatocellular carcinoma, *Oncology letters* 15 (5) (2018) 7783–7793.
- [5] W. J. d. S. Diniz, F. Canduri, *Bioinformatics: an overview and its applications*, *Genet Mol Res* 16 (1) (2017).

- [6] R. Parmezan Bonidia, A. C. Ponce de Leon Ferreira de Carvalho, A. Rossi Paschoal, D. Sipoli Sanches, Selecting the most relevant features for the identification of long non-coding rnas in plants, in: 2019 8th Brazilian Conference on Intelligent Systems (BRACIS), 2019, pp. 539–544. doi:10.1109/BRACIS.2019.00100.
- [7] V. I. Jurtz, A. R. Johansen, M. Nielsen, J. J. Almagro Armenteros, H. Nielsen, C. K. S nderby, O. Winther, S. K. S nderby, An introduction to deep learning on biological sequence data: examples and solutions, *Bioinformatics* 33 (22) (2017) 3685–3690. doi:10.1093/bioinformatics/btx531.  
URL <https://doi.org/10.1093/bioinformatics/btx531>
- [8] S. Budach, A. Marsico, pysster: classification of biological sequences by learning sequence and structure motifs with convolutional neural networks, *Bioinformatics* 34 (17) (2018) 3035–3037. doi:10.1093/bioinformatics/bty222.
- [9] S. Min, B. Lee, S. Yoon, Deep learning in bioinformatics, *Briefings in Bioinformatics* 18 (5) (2016) 851–869. doi:10.1093/bib/bbw068.
- [10] Z. Chen, P. Zhao, F. Li, T. T. Marquez-Lago, A. Leier, J. Revote, Y. Zhu, D. R. Powell, T. Akutsu, G. I. Webb, K.-C. Chou, A. I. Smith, R. J. Daly, J. Li, J. Song, iLearn: an integrated platform and meta-learner for feature engineering, machine-learning analysis and modeling of DNA, RNA and protein sequence data, *Briefings in Bioinformatics* 21 (3) (2019) 1047–1057. doi:10.1093/bib/bbz041.
- [11] M. E. Maros, D. Capper, D. T. Jones, V. Hovestadt, A. von Deimling, S. M. Pfister, A. Benner, M. Zucknick, M. Sill, Machine learning workflows to estimate class probabilities for precision cancer diagnostics on dna methylation microarray data, *Nature Protocols* (2020) 1–34.
- [12] C. Ma, H. H. Zhang, X. Wang, Machine learning for big data analytics in plants, *Trends in Plant Science* 19 (12) (2014) 798 – 808. doi:<https://doi.org/10.1016/j.tplants.2014.08.004>.
- [13] J. Li, W. Liu, Puzzle of highly pathogenic human coronaviruses (2019-ncov), *Protein & Cell* (2020) 1–4.

- [14] D. Benvenuto, M. Giovanetti, A. Ciccozzi, S. Spoto, S. Angeletti, M. Ciccozzi, The 2019-new coronavirus epidemic: Evidence for virus evolution, *Journal of Medical Virology* 92 (4) (2020) 455–459. arXiv:<https://onlinelibrary.wiley.com/doi/pdf/10.1002/jmv.25688>, doi:10.1002/jmv.25688. URL <https://onlinelibrary.wiley.com/doi/abs/10.1002/jmv.25688>
- [15] C. Xu, S. A. Jackson, BioSeq-Analysis: a platform for DNA, RNA and protein sequence analysis based on machine learning approaches, *Genome Biology* 20 (2019) 1–4. doi:<https://doi.org/10.1186/s13059-019-1689-0>. URL <https://doi.org/10.1186/s13059-019-1689-0>
- [16] D. Storcheus, A. Rostamizadeh, S. Kumar, A survey of modern questions and challenges in feature extraction, in: *Feature Extraction: Modern Questions and Challenges*, 2015, pp. 1–18.
- [17] R. Saidi, S. Aridhi, E. M. Nguifo, M. Maddouri, Feature extraction in protein sequences classification: a new stability measure, in: *Proceedings of the ACM Conference on Bioinformatics, Computational Biology and Biomedicine*, ACM, 2012, pp. 683–689.
- [18] I. Guyon, S. Gunn, M. Nikravesh, L. A. Zadeh, *Feature extraction: foundations and applications*, Vol. 207, Springer, 2008.
- [19] J. Baek, B. Lee, S. Kwon, S. Yoon, Incrnanet: Long non-coding rna identification using deep learning, *Bioinformatics* 1 (2018) 9.
- [20] R. P. Bonidia, L. D. H. Sampaio, F. M. Lopes, D. S. Sanches, Feature extraction of long non-coding rnas: A fourier and numerical mapping approach, in: I. Nyström, Y. Hernández Heredia, V. Milián Núñez (Eds.), *Progress in Pattern Recognition, Image Analysis, Computer Vision, and Applications*, Springer International Publishing, Cham, 2019, pp. 469–479.
- [21] X. Pan, K. Xiong, Predcircrna: computational classification of circular rna from other long non-coding rna using hybrid features, *Molecular Biosystems* 11 (8) (2015) 2219–2226.
- [22] R. Muhammad, S. Ahmed, D. Md Farid, S. Shatabda, A. Sharma, A. Dehhangi, PyFeat: a Python-based effective feature generation tool



- for DNA, RNA and protein sequences, *Bioinformatics* 35 (19) (2019) 3831–3833. arXiv:<http://oup.prod.sis.lan/bioinformatics/article-pdf/35/19/3831/30061688/btz165.pdf>, doi:10.1093/bioinformatics/btz165. URL <https://doi.org/10.1093/bioinformatics/btz165>
- [23] Q. Abbas, S. M. Raza, A. A. Biyabani, M. A. Jaffar, A review of computational methods for finding non-coding rna genes, *Genes* 7 (12) (2016) 113.
- [24] N. Amin, A. McGrath, Y.-P. P. Chen, Evaluation of deep learning in non-coding rna classification, *Nature Machine Intelligence* 1 (5) (2019) 246.
- [25] Y.-J. Kang, D.-C. Yang, L. Kong, M. Hou, Y.-Q. Meng, L. Wei, G. Gao, Cpc2: a fast and accurate coding potential calculator based on sequence intrinsic features, *Nucleic acids research* 45 (W1) (2017) W12–W16.
- [26] S. Han, Y. Liang, Q. Ma, Y. Xu, Y. Zhang, W. Du, C. Wang, Y. Li, Lncfinder: an integrated platform for long non-coding rna identification utilizing sequence intrinsic composition, structural information and physicochemical property, *Briefings in Bioinformatics* (2018).
- [27] L. Chen, Y.-H. Zhang, G. Huang, X. Pan, S. Wang, T. Huang, Y.-D. Cai, Discriminating circrnas from other lncrnas using a hierarchical extreme learning machine (h-elm) algorithm with feature selection, *Molecular Genetics and Genomics* 293 (1) (2018) 137–149.
- [28] J. J. Quinn, H. Y. Chang, Unique features of long non-coding rna biogenesis and function, *Nature Reviews Genetics* 17 (1) (2016) 47.
- [29] S. R. Eddy, Non-coding rna genes and the modern rna world, *Nature Reviews Genetics* 2 (12) (2001) 919.
- [30] P. Kapranov, J. Cheng, S. Dike, D. A. Nix, R. Dutttagupta, A. T. Willingham, P. F. Stadler, J. Hertel, J. Hackermüller, I. L. Hofacker, et al., Rna maps reveal new rna classes and a possible function for pervasive transcription, *Science* 316 (5830) (2007) 1484–1488.
- [31] Y. Zhang, Y. Tao, Q. Liao, Long noncoding rna: a crosslink in biological regulatory network, *Briefings in bioinformatics* (2017).

- [32] A. Li, Q. Zang, D. Sun, M. Wang, A text feature-based approach for literature mining of lncrna–protein interactions, *Neurocomputing* 206 (2016) 73–80.
- [33] Y. Wang, Y. Li, Q. Wang, Y. Lv, S. Wang, X. Chen, X. Yu, W. Jiang, X. Li, Computational identification of human long intergenic non-coding rnas using a ga–svm algorithm, *Gene* 533 (1) (2014) 94–99.
- [34] L. Wang, L. Kuang, S. Ye, M. F. B. Iqbal, T. Pei, et al., A novel method for lncrna-disease association prediction based on an lncrna-disease association network, *IEEE/ACM Transactions on Computational Biology and Bioinformatics* (2018).
- [35] W. Zhang, Q. Qu, Y. Zhang, W. Wang, The linear neighborhood propagation method for predicting long non-coding rna–protein interactions, *Neurocomputing* 273 (2018) 526–534.
- [36] Q.-Z. Zhou, B. Zhang, Q.-Y. Yu, Z. Zhang, Bmncrnadb: a comprehensive database of non-coding rnas in the silkworm, *bombyx mori*, *BMC bioinformatics* 17 (1) (2016) 370.
- [37] M. Q. Hassan, C. E. Tye, G. S. Stein, J. B. Lian, Non-coding rnas: Epigenetic regulators of bone development and homeostasis, *Bone* 81 (2015) 746–756.
- [38] C. Ciaudo, N. Servant, V. Cognat, A. Sarazin, E. Kieffer, S. Viville, V. Colot, E. Barillot, E. Heard, O. Voinnet, Highly dynamic and sex-specific expression of micrnas during early es cell differentiation, *PLoS genetics* 5 (8) (2009) e1000620.
- [39] X. Peng, L. Gralinski, C. D. Armour, M. T. Ferris, M. J. Thomas, S. Proll, B. G. Bradel-Tretheway, M. J. Korth, J. C. Castle, M. C. Biery, et al., Unique signatures of long noncoding rna expression in response to virus infection and altered innate immune signaling, *MBio* 1 (5) (2010) e00206–10.
- [40] C. Pastori, C. Wahlestedt, Involvement of long noncoding rnas in diseases affecting the central nervous system, *RNA biology* 9 (6) (2012) 860–870.

- [41] Q. Zhang, Y. Wei, Z. Yan, C. Wu, Z. Chang, Y. Zhu, K. Li, Y. Xu, The characteristic landscape of lncrnas classified by rbp–lncrna interactions across 10 cancers, *Molecular bioSystems* 13 (6) (2017) 1142–1151.
- [42] H.-L. V. Wang, J. A. Chekanova, Long noncoding rnas in plants, in: *Long Non Coding RNA Biology*, Springer, 2017, pp. 133–154.
- [43] C. Di, J. Yuan, Y. Wu, J. Li, H. Lin, L. Hu, T. Zhang, Y. Qi, M. B. Gerstein, Y. Guo, et al., Characterization of stress-responsive lncrnas in arabidopsis thaliana by integrating expression, epigenetic and structural features, *The Plant Journal* 80 (5) (2014) 848–861.
- [44] D. Wang, Z. Qu, L. Yang, Q. Zhang, Z.-H. Liu, T. Do, D. L. Adelson, Z.-Y. Wang, I. Searle, J.-K. Zhu, Transposable elements (te s) contribute to stress-related long intergenic noncoding rna s in plants, *The Plant Journal* 90 (1) (2017) 133–146.
- [45] Y.-C. Zhang, J.-Y. Liao, Z.-Y. Li, Y. Yu, J.-P. Zhang, Q.-F. Li, L.-H. Qu, W.-S. Shu, Y.-Q. Chen, Genome-wide screening and functional analysis identify a large number of long noncoding rnas involved in the sexual reproduction of rice, *Genome biology* 15 (12) (2014) 512.
- [46] Y. Fang, M. J. Fullwood, Roles, functions, and mechanisms of long non-coding rnas in cancer, *Genomics, proteomics & bioinformatics* 14 (1) (2016) 42–54.
- [47] T. Derrien, R. Johnson, G. Bussotti, A. Tanzer, S. Djebali, H. Tilgner, G. Guernec, D. Martin, A. Merkel, D. G. Knowles, et al., The genecode v7 catalog of human long noncoding rnas: analysis of their gene structure, evolution, and expression, *Genome research* 22 (9) (2012) 1775–1789.
- [48] J. Cheng, P. Kapranov, J. Drenkow, S. Dike, S. Brubaker, S. Patel, J. Long, D. Stern, H. Tamma, G. Helt, et al., Transcriptional maps of 10 human chromosomes at 5-nucleotide resolution, *Science* 308 (5725) (2005) 1149–1154.
- [49] L. Ma, V. B. Bajic, Z. Zhang, On the classification of long non-coding rnas, *RNA biology* 10 (6) (2013) 924–933.

- [50] R. Hu, X. Sun, Incrnatargets: a platform for lncrna target prediction based on nucleic acid thermodynamics, *Journal of bioinformatics and computational biology* 14 (04) (2016) 1650016.
- [51] S. Chooniedass-Kothari, E. Emberley, M. Hamedani, S. Troup, X. Wang, A. Czosnek, F. Hube, M. Mutawe, P. Watson, E. Leygue, The steroid receptor rna activator is the first functional rna encoding a protein, *FEBS letters* 566 (1-3) (2004) 43–47.
- [52] Y. He, X.-M. Meng, C. Huang, B.-M. Wu, L. Zhang, X.-W. Lv, J. Li, Long noncoding rnas: Novel insights into hepatocellular carcinoma, *Cancer letters* 344 (1) (2014) 20–27.
- [53] J. T. Kung, D. Colognori, J. T. Lee, Long noncoding rnas: past, present, and future, *Genetics* 193 (3) (2013) 651–669.
- [54] L. Kong, Y. Zhang, Z.-Q. Ye, X.-Q. Liu, S.-Q. Zhao, L. Wei, G. Gao, Cpc: assess the protein-coding potential of transcripts using sequence features and support vector machine, *Nucleic acids research* 35 (suppl\_2) (2007) W345–W349.
- [55] L. Wang, H. J. Park, S. Dasari, S. Wang, J.-P. Kocher, W. Li, Cpat: Coding-potential assessment tool using an alignment-free logistic regression model, *Nucleic acids research* 41 (6) (2013) e74–e74.
- [56] L. Sun, H. Luo, D. Bu, G. Zhao, K. Yu, C. Zhang, Y. Liu, R. Chen, Y. Zhao, Utilizing sequence intrinsic composition to classify protein-coding and long non-coding transcripts, *Nucleic acids research* 41 (17) (2013) e166–e166.
- [57] A. Li, J. Zhang, Z. Zhou, Plek: a tool for predicting long non-coding rnas and messenger rnas based on an improved k-mer scheme, *BMC bioinformatics* 15 (1) (2014) 311.
- [58] X.-N. Fan, S.-W. Zhang, Incrna-mfdl: identification of human long non-coding rnas by fusing multiple features and using deep learning, *Molecular BioSystems* 11 (3) (2015) 892–897.
- [59] R. Achawanantakun, J. Chen, Y. Sun, Y. Zhang, Lncrna-id: Long non-coding rna identification using balanced random forests, *Bioinformatics* 31 (24) (2015) 3897–3905.

- [60] L. Sun, H. Liu, L. Zhang, J. Meng, Incrscan-svm: a tool for predicting long non-coding rnas using support vector machine, *PloS one* 10 (10) (2015) e0139654.
- [61] C. Pian, G. Zhang, Z. Chen, Y. Chen, J. Zhang, T. Yang, L. Zhang, Lncrnared: Classification of long non-coding rnas and protein-coding transcripts by the ensemble algorithm with a new hybrid feature, *PloS one* 11 (5) (2016) e0154567.
- [62] R. Tripathi, S. Patel, V. Kumari, P. Chakraborty, P. K. Varadwaj, Deeplnc, a long non-coding rna prediction tool using deep neural network, *Network Modeling Analysis in Health Informatics and Bioinformatics* 5 (1) (2016) 21.
- [63] L. M. Vieira, C. Grativol, F. Thiebaut, T. G. Carvalho, P. R. Haridoim, A. Hemerly, S. Lifschitz, P. C. G. Ferreira, M. E. M. Walter, Plantrna.sniffer: a svm-based workflow to predict long intergenic non-coding rnas in plants, *Non-coding RNA* 3 (1) (2017) 11.
- [64] U. Singh, N. Khemka, M. S. Rajkumar, R. Garg, M. Jain, Plncpro for prediction of long non-coding rnas (lncrnas) in plants and its application for discovery of abiotic stress-responsive lncrnas in rice and chickpea, *Nucleic acids research* 45 (22) (2017) e183–e183.
- [65] T. d. C. Negri, W. A. L. Alves, P. H. Bugatti, P. T. M. Saito, D. S. Domingues, A. R. Paschoal, Pattern recognition analysis on long non-coding rnas: a tool for prediction in plants, *Briefings in bioinformatics* (2018).
- [66] E. A. Ito, I. Katahira, F. F. d. R. Vicente, L. F. P. Pereira, F. M. Lopes, Basinet—biological sequences network: a case study on coding and non-coding rnas identification, *Nucleic acids research* (2018).
- [67] C. M. Simopoulos, E. A. Weretilnyk, G. B. Golding, Prediction of plant lncrna by ensemble machine learning classifiers, *BMC genomics* 19 (1) (2018) 316.
- [68] J.-C. Guo, S.-S. Fang, Y. Wu, J.-H. Zhang, Y. Chen, J. Liu, B. Wu, J.-R. Wu, E.-M. Li, L.-Y. Xu, L. Sun, Y. Zhao, CNIT: a fast and accurate web tool for identifying protein-coding and long non-coding

- transcripts based on intrinsic sequence composition, *Nucleic Acids Research* 47 (W1) (2019) W516–W522. doi:10.1093/nar/gkz400.
- [69] S. Deshpande, J. Shuttleworth, J. Yang, S. Taramonli, M. England, Plit: An alignment-free computational tool for identification of long non-coding rnas in plant transcriptomic datasets, *Computers in Biology and Medicine* 105 (2019) 169 – 181. doi:<https://doi.org/10.1016/j.combiomed.2018.12.014>.
- [70] S. Liu, X. Zhao, G. Zhang, W. Li, F. Liu, S. Liu, W. Zhang, Predlnc-gfstack: A global sequence feature based on a stacked ensemble learning method for predicting lncrnas from transcripts, *Genes* 10 (9) (2019) 672.
- [71] G. Wang, H. Yin, B. Li, C. Yu, F. Wang, X. Xu, J. Cao, Y. Bao, L. Wang, A. A. Abbasi, V. B. Bajic, L. Ma, Z. Zhang, Characterization and identification of long non-coding RNAs based on feature relationship, *Bioinformatics* 35 (17) (2019) 2949–2956. doi:10.1093/bioinformatics/btz008.
- [72] Y. Zhang, C. Jia, M. J. Fullwood, C. K. Kwoh, DeepCPP: a deep neural network based on nucleotide bias information and minimum distribution similarity feature selection for RNA coding potential prediction, *Briefings in Bioinformatics* (03 2020). doi:10.1093/bib/bbaa039.
- [73] S. F. Altschul, T. L. Madden, A. A. Schäffer, J. Zhang, Z. Zhang, W. Miller, D. J. Lipman, Gapped blast and psi-blast: a new generation of protein database search programs, *Nucleic acids research* 25 (17) (1997) 3389–3402.
- [74] A. C. Liu, The effect of oversampling and undersampling on classifying imbalanced text datasets, The University of Texas at Austin (2004).
- [75] D. M. Goodstein, S. Shu, R. Howson, R. Neupane, R. D. Hayes, J. Fazo, T. Mitros, W. Dirks, U. Hellsten, N. Putnam, et al., Phytozome: a comparative platform for green plant genomics, *Nucleic acids research* 40 (D1) (2011) D1178–D1186.
- [76] A. Paytuví Gallart, A. Hermoso Pulido, I. Anzar Martínez de Lagrán, W. Sanseverino, R. Aiese Cigliano, Greenc: a wiki-based database of plant lncrnas, *Nucleic acids research* 44 (D1) (2015) D1161–D1166.

- [77] D. Chen, C. Yuan, J. Zhang, Z. Zhang, L. Bai, Y. Meng, L.-L. Chen, M. Chen, PlantNATsDB: a comprehensive database of plant natural antisense transcripts, *Nucleic Acids Research* 40 (D1) (2011) D1187–D1193. arXiv:<https://academic.oup.com/nar/article-pdf/40/D1/D1187/9481672/gkr823.pdf>, doi:10.1093/nar/gkr823. URL <https://doi.org/10.1093/nar/gkr823>
- [78] Q. Chu, X. Zhang, X. Zhu, C. Liu, L. Mao, C. Ye, Q.-H. Zhu, L. Fan, Plantcircbase: a database for plant circular rnas, *Molecular plant* 10 (8) (2017) 1126–1128.
- [79] C. Yin, Y. Chen, S. S.-T. Yau, A measure of dna sequence similarity by fourier transform with applications on hierarchical clustering, *Journal of theoretical biology* 359 (2014) 18–28.
- [80] C. Yin, S. S.-T. Yau, A fourier characteristic of coding sequences: origins and a non-fourier approximation, *Journal of computational biology* 12 (9) (2005) 1153–1165.
- [81] D. Anastassiou, Genomic signal processing, *IEEE signal processing magazine* 18 (4) (2001) 8–20.
- [82] L. Marsella, F. Sirocco, A. Trovato, F. Seno, S. C. Tosatto, Repetita: detection and discrimination of the periodicity of protein solenoid repeats by discrete fourier transform, *Bioinformatics* 25 (12) (2009) i289–i295.
- [83] W. T. Cochran, J. W. Cooley, D. L. Favin, H. D. Helms, R. A. Kaenel, W. W. Lang, G. C. Maling, D. E. Nelson, C. M. Rader, P. D. Welch, What is the fast fourier transform?, *Proceedings of the IEEE* 55 (10) (1967) 1664–1674.
- [84] M. Abo-Zahhad, S. M. Ahmed, S. A. Abd-Elrahman, Genomic analysis and classification of exon and intron sequences using dna numerical mapping techniques, *International Journal of Information Technology and Computer Science* 4 (8) (2012) 22–36.
- [85] G. Mendizabal-Ruiz, I. Román-Godínez, S. Torres-Ramos, R. A. Salido-Ruiz, J. A. Morales, On dna numerical representations for genomic similarity computation, *PloS one* 12 (3) (2017) e0173288.

- [86] R. F. Voss, Evolution of long-range fractal correlations and  $1/f$  noise in dna base sequences, *Physical review letters* 68 (25) (1992) 3805.
- [87] P. D. Cristea, Conversion of nucleotides sequences into genomic signals, *Journal of cellular and molecular medicine* 6 (2) (2002) 279–303.
- [88] N. Chakravarthy, A. Spanias, L. D. Iasemidis, K. Tsakalis, Autoregressive modeling and feature analysis of dna sequences, *EURASIP Journal on Applied Signal Processing* 2004 (2004) 13–28.
- [89] R. Zhang, C.-T. Zhang, Z curves, an intuitive tool for visualizing and analyzing the dna sequences, *Journal of Biomolecular Structure and Dynamics* 11 (4) (1994) 767–782.
- [90] A. S. Nair, S. P. Sreenadhan, A coding measure scheme employing electron-ion interaction pseudopotential (eiip), *Bioinformation* 1 (6) (2006) 197.
- [91] D. Anastassiou, Genomic signal processing, *IEEE Signal Processing Magazine* 18 (4) (2001) 8–20. doi:10.1109/79.939833.
- [92] N. Yu, Z. Li, Z. Yu, Survey on encoding schemes for genomic data representation and feature learning—from signal processing to machine learning, *Big Data Mining and Analytics* 1 (3) (2018) 191–210.
- [93] J. Shao, X. Yan, S. Shao, Snr of dna sequences mapped by general affine transformations of the indicator sequences, *Journal of mathematical biology* 67 (2) (2013) 433–451.
- [94] C.-T. Zhang, A symmetrical theory of dna sequences and its applications, *Journal of theoretical biology* 187 (3) (1997) 297–306.
- [95] C. Yin, S. S.-T. Yau, Prediction of protein coding regions by the 3-base periodicity analysis of a dna sequence, *Journal of theoretical biology* 247 (4) (2007) 687–694.
- [96] H. Nikookar, Peak-to-average power ratio, in: *Wavelet Radio: Adaptive and Reconfigurable Wireless Systems Based on Wavelets*, Cambridge University Press, 2013, pp. 93–111. doi:10.1017/CBO9781139084697.006.



- [97] I. Pritišanac, R. M. Vernon, A. M. Moses, J. D. Forman Kay, Entropy and information within intrinsically disordered protein regions, *Entropy* 21 (7) (2019) 662.
- [98] S. Vinga, Information theory applications for biological sequence analysis, *Briefings in bioinformatics* 15 (3) (2013) 376–389.
- [99] J. T. Machado, A. C. Costa, M. D. Quelhas, Shannon, rényie and tsallis entropy analysis of dna using phase plane, *Nonlinear Analysis: Real World Applications* 12 (6) (2011) 3135–3144.
- [100] A. Lesne, Shannon entropy: a rigorous notion at the crossroads between probability, information theory, dynamical systems and statistical physics, *Mathematical Structures in Computer Science* 24 (3) (2014).
- [101] M. P. De Albuquerque, I. A. Esquef, A. G. Mello, Image thresholding using tsallis entropy, *Pattern Recognition Letters* 25 (9) (2004) 1059–1065.
- [102] F. M. Lopes, E. A. de Oliveira, R. M. Cesar, Inference of gene regulatory networks from time series by tsallis entropy, *BMC systems biology* 5 (1) (2011) 61.
- [103] A. Ramírez-Reyes, A. R. Hernández-Montoya, G. Herrera-Corral, I. Domínguez-Jiménez, Determining the entropic index  $q$  of tsallis entropy in images through redundancy, *Entropy* 18 (8) (2016) 299.
- [104] L. d. F. Costa, F. A. Rodrigues, A. S. Cristino, Complex networks: the key to systems biology, *Genetics and Molecular Biology* 31 (3) (2008) 591–601.
- [105] X. F. Wang, Complex networks: topology, dynamics and synchronization, *International journal of bifurcation and chaos* 12 (05) (2002) 885–916.
- [106] B. K. Singh, K. Verma, A. Thoke, Investigations on impact of feature normalization techniques on classifier’s performance in breast tumor classification, *International Journal of Computer Applications* 116 (19) (2015).

- [107] M. C. de Souto, D. S. de Araujo, I. G. Costa, R. G. Soares, T. B. Ludermir, A. Schliep, Comparative study on normalization procedures for cluster analysis of gene expression datasets, in: Neural Networks, 2008. IJCNN 2008.(IEEE World Congress on Computational Intelligence). IEEE International Joint Conference on, IEEE, 2008, pp. 2792–2798.
- [108] L. Breiman, Random forests, Machine learning 45 (1) (2001) 5–32.
- [109] T. Hastie, S. Rosset, J. Zhu, H. Zou, Multi-class adaboost, Statistics and its Interface 2 (3) (2009) 349–360.
- [110] A. V. Dorogush, V. Ershov, A. Gulin, Catboost: gradient boosting with categorical features support, arXiv preprint arXiv:1810.11363 (2018).
- [111] J. Cohen, A coefficient of agreement for nominal scales, Educational and psychological measurement 20 (1) (1960) 37–46.